UNIVERSITÀ DEGLI STUDI DI PALERMO

Dottorato di Ricerca in Biomedicina e Neuroscienze

Dipartimento di Biomedicina, Neuroscienze e Diagnostica avanzata (BiND)

SSD BIO/16

Treatment with Nicotine-derived Nitrosamine Ketone (NNK) Causes Disruption of Blood Brain Barrier (BBB) and Microglia Activation in Mice

IL DOTTORE

Lorenzo Francisco Ochoa

IL COORDINATORE

Chiar.mo Prof. Fabio Bucchieri

IL TUTOR

Chiar.mo Prof. Fabio Bucchieri

LA CO-TUTOR

Chiar.ma Prof.ssa Gracie Vargas

CICLO XXXIV

ANNO CONSEGUIMENTO TITOLO 2022

“La irrealidad de lo mirado da realidad a la mirada.”

Octavio Paz

Index

Acknowledgments

I set sail to a future that was said not to belong to me, and I have just landed. And just like every voyage before, it is thanks to the crew that this was even a possibility.

-To Dr. Gracie Vargas for allowing me to take chances in a field foreign to me.

-To Rahul Pal for paying attention to my rambling in and out of the lab for years (past, present, and future).

-To Claudia Di Gesu for providing all the help of mentor while navigating the Italian system.

-To my committee members for providing guidance and support: Dr. Fabio Bucchieri, Dr. Bill Ameredes, Dr. Giulio Taglialatela, and Dr. Massoud Motamedi.

-To Jonathan Luisi for “nerding it out” with me about the nerdiest subjects there are.

-To Dr. Owen Hamill for noticing the effort I put into my work even when others didn’t.

-To Olivia Solomon, Fan Xia, and the many lab members I share space and knowledge with.

-To Dr. Jun-Ho La and Dr. Andres Oberhauser for generously proving their time to review my thesis.

-To my mother, my father, my sister, and my brother for believing in me.

-To PPP for giving me that hand when I needed it.

-To those that didn’t believe in me for giving me fuel to prove them wrong.

-And to Paula Villarreal for sharing her life with me and blaming me for dropping the juice.

List of Abbreviations

- 2P – 2 photon
- 7-mGua - 7-N-methylguanine
- 8-OHdG - 8-hydroxy-2'-deoxyguanosine
- AD - Alzheimer’s disease
- APP - amyloid precursor protein
- Aβ - amyloid β
- BBB – blood brain barrier
- BBMEC - bovine brain microvessel endothelial cells
- CNS - central nervous system
- COPD - chronic obstructive pulmonary disease
- CS – cigarette smoke
- CVD - cardiovascular diseases
- DMSO – dimethyl sulfoxide
- eGFP – enhanced fluorescence protein
- ENOS - endothelial citric oxide synthase
- FOV – field of view
- IP – intraperitoneal
- IVM – intravital microscopy

- ML – machine learning
- MPM – multiphoton microscopy
- MRI – magnetic resonance imaging
- nAChRs - nicotinic acetylcholine receptors
- NNAL - 4-(methylnitrosamino)-1-(3-pyridyl)-1-butanol
- NNK - 4-Methylnitrosamino-1-(3-pyridyl)-1-butanone
- NNN - N'-Nitrosonornicotine
- NO – nitric oxide
- O4-mTh - O^4-methylthymine
- O6-mGua - O^6-methylguanine
- OC – optical clearing
- OxS – oxidative stress
- P-450 - cytochrome P-450
- PD - Parkinson's disease
- PET – positron emission tomography
- PHA - polycyclic aromatic hydrocarbons
- PPP - pentose phosphate pathway
- ROI – region of interest
- ROS – reactive oxygen species

- SHG – second harmonic generation
- SVID - small vessel ischemic disease
- TDE - 2,2′-Thiodiethanol
- Ti:sapphire – titanium-sapphire
- TJ - thigh junctions
- VAM - vessel associated microglia
- WEKA - Waikato Environment for Knowledge Analysis
- ZO-1 - zonula occludens-1
- α7nAChRs - α7 homomeric nicotinic acetylcholine receptors
- β-AdrRs - β-adrenergic receptors

List of Figures and Tables

Chapter I

Chapter II Figures

114

Abstract

4-Methylnitrosamino-1-(3-pyridyl)-1-butanone (NNK) is a nicotine metabolite produced within the tobacco plant, from combustion, and from metabolic breakdown. Cigarette Smoke (CS) continues to be a leading cause for decline of quality of life as well as deaths globally. While the link to poor health and eventually early death has been accepted for decades, it is increasingly recognized that smoking may contribute to a broad range of disorders. Epidemiologically, CS has been associated with neuroinflammation and several neurological disorders including Alzheimer's disease, stroke, and multiple sclerosis. While direct links are not fully understood, studies in a humanized flow-based *in vitro* blood-brain barrier model used CS extract to show that CS can have pro-inflammatory effects and promote loss of BBB function and viability. Moreover, other studies have found that CS extract exacerbates hyperpermeability of cerebral endothelial pointing to disruption of the integrity of the BBB. CS is also linked to increased oxidative stress in neurons, microglia, and astrocytes in both *in vivo* and preclinical models. In one study, NNK was suggested to induce glial activation sustained from 4 to 12 days when given IP in mice. While studies of the direct effects of CS are valuable the composition of chemicals is complex and highly variable. Another approach is to study the effect of a prominent component. Extensive cancer literature has established NNK as an important component of CS for having a direct effect on DNA mutation and its ability to bind and activate nicotinic acetylcholine receptors (nAChRs). However, little is known about the specific effects of NNK on the BBB or microglial dynamics particularly as they relate to the vasculature and across multiple areas. Here we show that NNK when given through an intranasal route, both in acute (4 days) and chronic (12 weeks) exposures, leads to both disruption of the BBB and vessel-localized microglia activation that is highly localized to the vasculature, the latter of which shows increased vasospastic activity. To investigate microglial and vascular responses to intranasal NNK *in vivo*, we combined the use of a transgenic mouse line (CX3CR1-GFP) with intravital neuroimaging. Single volumetric images and time series of up to an hour were taken to assess spatial and dynamic observations.

A machine learning algorithm was employed to segment microglial soma from processes and analyses were performed to evaluate morphometry as well as associations with the vasculature. Results indicate that microglia activation was found to be heterogeneous; that is activated microglia and ramified microglia existed within the same field of view with activated glia in contact or localized to the vasculature. NNK-treated animals displayed a quantitative increase in vessel-associated microglia (VAM) compared to PBS controls. Temporal analysis in those sites showed VAM microglial sustained an ameboid appearance over time and clustered near the vessels. An increase in vascular events, including vasoconstriction, vasodilation, and microbursts, were observed in NNK-treated animals suggesting a pronounced effect of NNK in vasculature. In chronic treatment, the mentioned effects were sustained and in some cases exacerbated. Taken together, these results suggest an immunomodulatory effect of NNK marked by sporadic and highly localized microglia activity accompanied by vascular events which over the long term can produce pathophysiology that could contribute to or exacerbate ongoing or developing disease processes. This work lays the groundwork for studies that examine the potential role of other components in cigarettes or e-cigs as it relates to neurological disorders.

Chapter I

Introduction

It has been long known that cigarette smoke (CS) is associated with lung disease, coronary heart disease, and complications in pregnancy[1, 2] but more recently effects on the brain have been discovered with research showing an association with neuroinflammation and several neurological disorders[3-5]. CS is made up of a horde of chemicals, including nitrosamines, heavy metals, and reactive oxygen species (ROS)[6], that quickly flux into the nasal and oral mucosa, the lining of the epithelial airway, and ultimately spread into body tissues, through blood circulation. These different CS toxins have immunomodulatory effects, which in turn trigger inflammatory mediators, like cytokines and chemokines that can lead to neuroinflammation[5, 7]. It should be noted that deleterious effects of CS and its constituents occur despite the potentially protective effects of nicotine[8]. Recent studies have also indicated that chemicals, such as nitrosamines, in CS (and incidentally, also found in electronic cigarettes) specifically lead to neuroinflammation with effects that could contribute to the development of neurodegenerative disorders like Alzheimer's disease (AD)[9,14].

1.1 Detrimental Effects of Cigarette Smoke

CS is the leading cause of cancer-related death in the world, and it's associated with approximately 480,000 deaths per year in the United States, including more than 41,000 deaths resulting from secondhand smoke exposure (CDC, 2020). Combustion of tobacco contained in cigarettes comprises of at least 7000 chemicals, including polycyclic aromatic hydrocarbons (PAHs), volatile hydrocarbons, aromatic amines, aldehydes, phenols, nitro compounds, N-nitrosamines, of which many have been linked to deleterious effects such as the development of cancer, chronic obstructive pulmonary disease (COPD), and stroke.[10 11] While nicotine is generally accepted as non-carcinogenic, new evidence suggests that it can be bio-converted within the cell into dangerous metabolites that include the nitrosamine 4-methylnitrosamino-1-(3-pyridyl)-1-butanone (NNK) known for its carcinogenic effects. Nicotine, and its metabolites such as

NNK, also promotes cancer by activating signaling pathways facilitating cancer cell growth, angiogenesis, migration, and invasion.[10]

CS has been shown to lead to cancer through multiple pathways. These include: (1) the direct exposure to carcinogens (e.g., PAHs & N-nitrosamines), (2) the formation of DNA adducts, and (3) the accumulation of permanent somatic mutations in critical genes (Fig. 1). A number of carcinogens in CS require conversion into active forms of the compounds through enzymatic activity within the cell. One example of such metabolic activation through enzymes is the conversion of CS compounds by cytochrome P-450 enzymes (P-450s) .[12] P-450 converts compounds present in CS into forms that can covalently bind to DNA and form DNA adducts. These specific types of enzymes have been shown to catalyze reactions of PAHs and induce metabolic activation.[13] Additionally, P-450s are inducible by other compounds including isotype specificity.[12]These enzymes are central to cancer formation and therefore as targets in cancer treatment.[14]

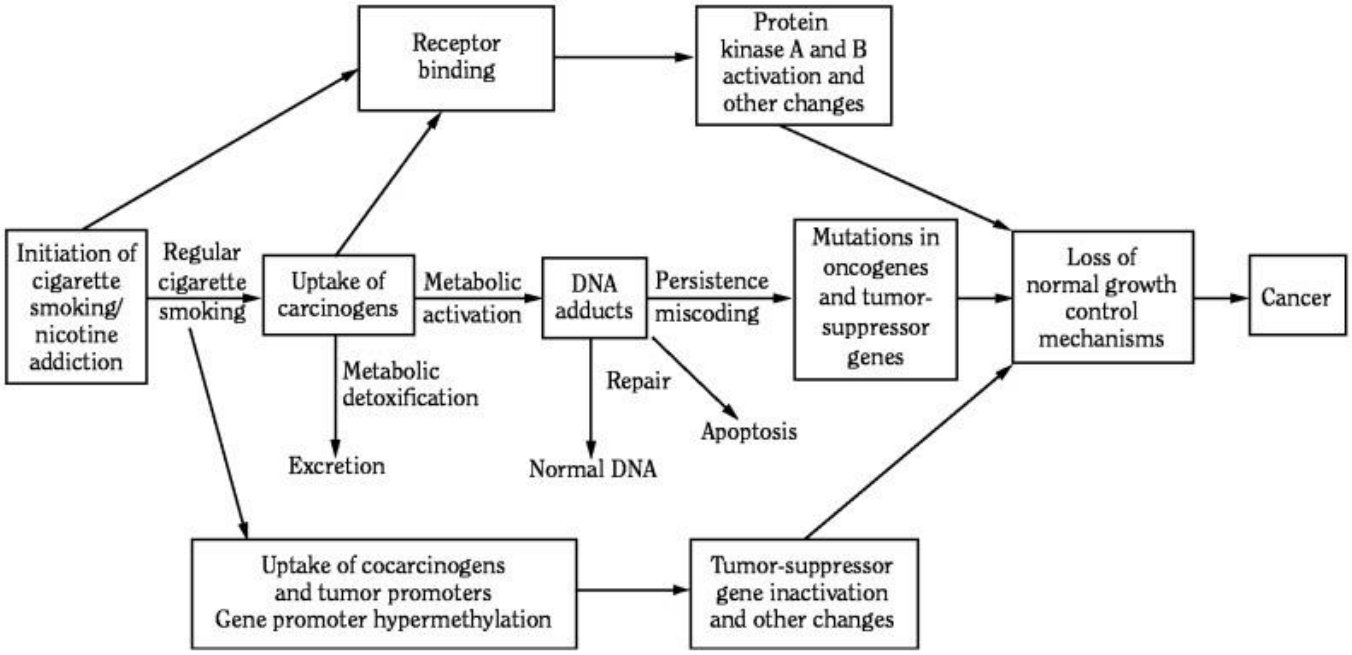

Figure 1[12]: Link between cigarette smoking and cancer through carcinogens in tobacco smoke. Adapted from the Surgeon General Report 2010.

Metabolic activation of CS compounds plays a central role in cancer formation. However, certain compounds can form DNA adducts without activation through enzymes. These include the nitrosamine class of compounds readily found in CS. It is well established that nicotine can undergo chemical conversions into NNK, N'-Nitrosonornicotine (NNN), and 4-(methylnitrosamino)-1-(3-pyridyl)-1-butanol (NNAL).[15] Catalyze-independent conversion of nicotine into nitrosamines can then lead to DNA adducts (Fig. 2).[15] Nicotine and nitrosamines (i.e., NNK, NNN,) are also implicated in tumor promotion by activating nicotinic acetylcholine receptors (nAChRs) and β-adrenergic receptors (β-AdrRs), leading to downstream activation of parallel signal transduction pathways that facilitate tumor progression.[12]

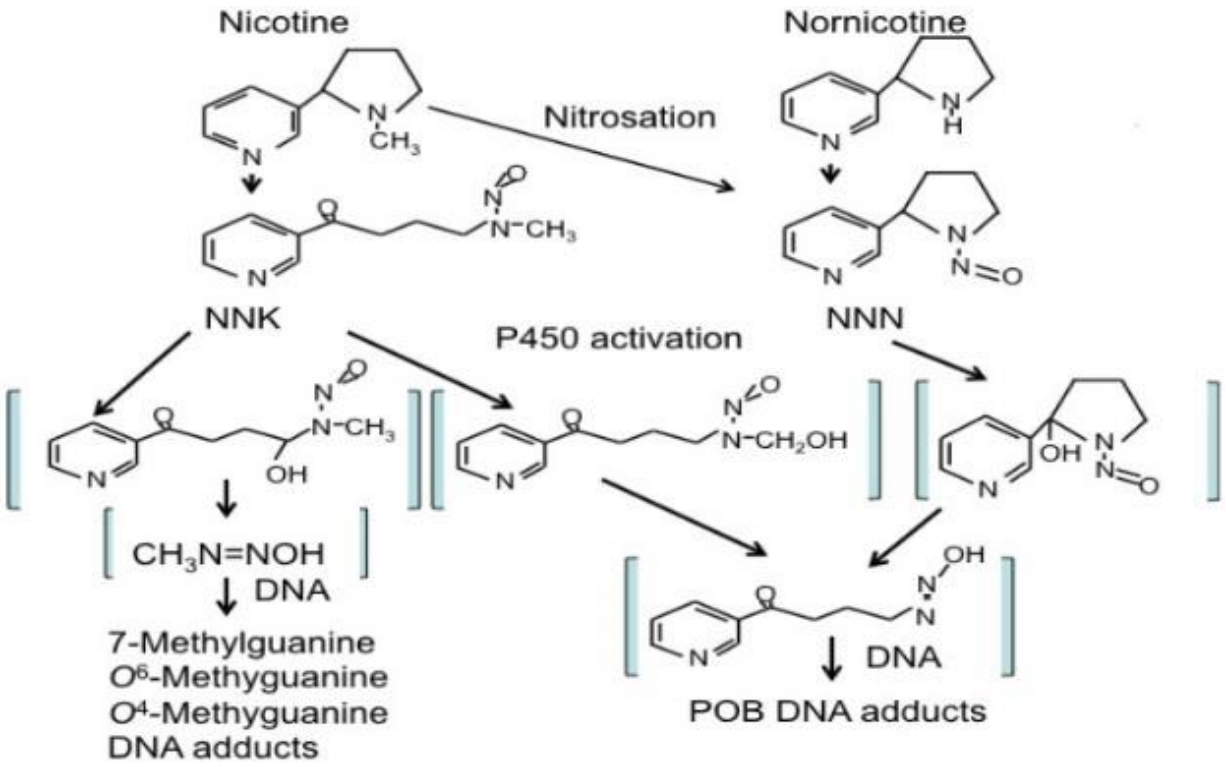

Figure 2: Schematic illustration of the pathways of NNK and NNN metabolism and DNA adduct formation as determined by studies in laboratory animals and humans. NNK: 4-(methylnitrosamino)-1-(3-pyridyl)-1-butanone, NNN: N'-nitrosonornicotine. Adapted from Xue et al, 2014.[15]

Compelling evidence point to higher DNA adduct levels in samples from CS users than in corresponding tissues of nonsmokers.[16] Thus it is believed that DNA adduct formation is one of the major pathways in which cancer formation occurs in CS users. Propagation of such damage with repeated exposure to CS, as is the case with typical nicotine product usage, explains the high incidence, and variety, of cancers in CS users. In addition, the continuous activation of nAChRs and subsequent increased metabolic demand provide an optimal environment for the development of cancers.

1.2 Cigarette Smoke and Oxidative Stress (OxS)

CS has been well established to exert effects throughout the body with damaging effects on the cardiovascular and respiratory systems. As CS is rarely precise in terms of exposure for both content and route, multiple organ systems can be affected at different time frames with different outcomes. The respiratory system tends to be one of the most severely affected systems by CS exposure. This system is comprised of the nose, pharynx, larynx, trachea, bronchi, and bronchioles. Inhaled CS moves through the respiratory system in that order where more soluble gases are adsorbed, and particles are deposited in the airways and alveoli. Due to the nature of tobacco smoking pattern of use, insults are of a repetitive and sustained nature that decreases the chances of repair process resulting in scar tissue which locally stiffens its structure, and over time leads to a serious loss of lung function and increasing morbidities.[17] Most notably, CS has been linked to about 80% to 90% of lung cancer deaths in the United States .[12] These statistics only included firsthand smoking and exclude potential damages from second and third-hand smoke. As previously discussed, the mechanism of CS that lead to cancer has extensively been studied. However, other molecular targets and mechanisms exist outside of its pro-cancer effects. Moreover, CS exposure can lead to increased susceptibility to infections due to structural changes and immunomodulatory effects it exerts on lung tissue.[18] Remarkably, the ability of CS to increase OxS burden has received limited attention.

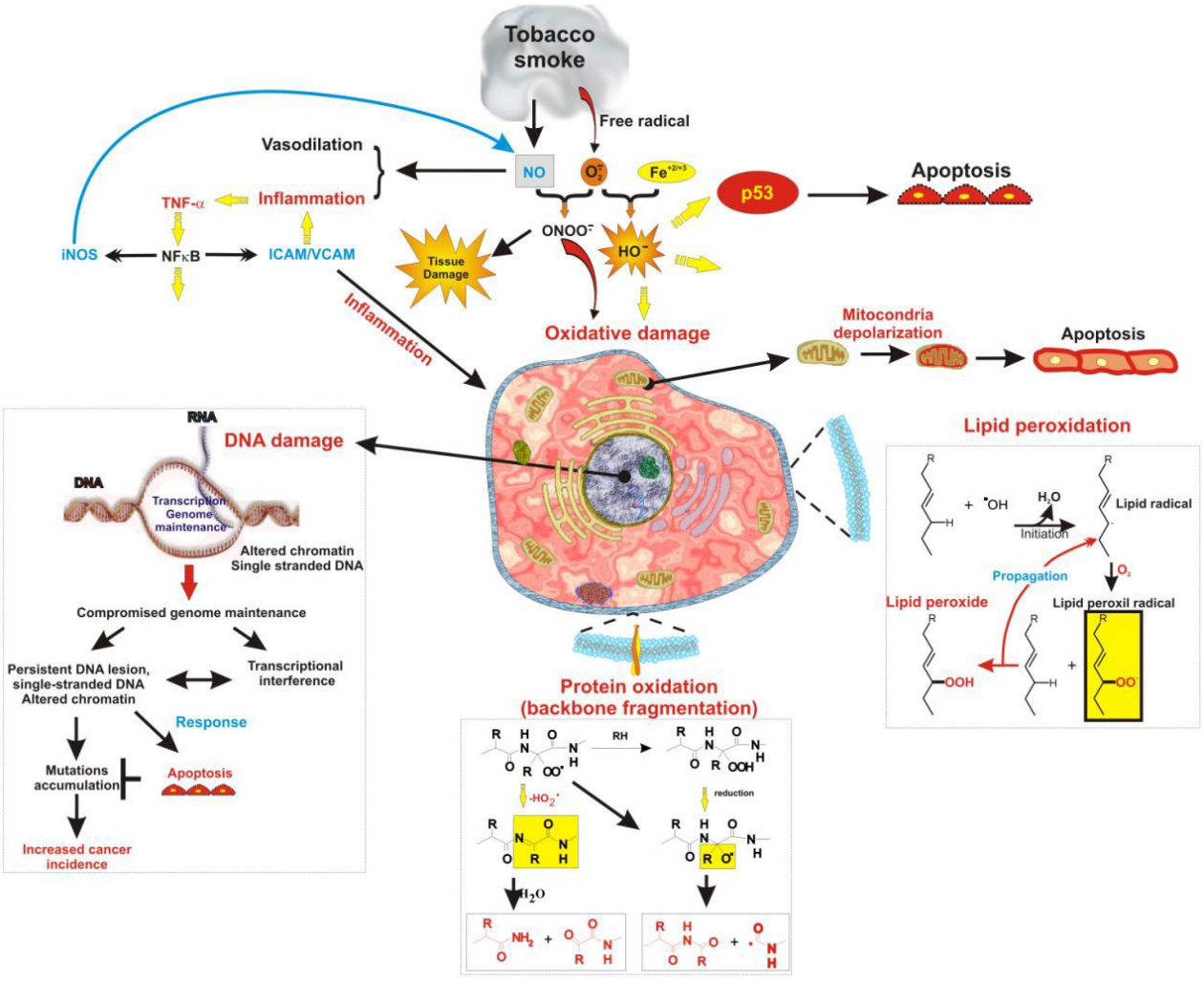

Figure 3:[6] Cellular response to OxS induced by tobacco smoke. Oxidative damage from CS can affect multiple pathways including DNA damage, protein oxidation, lipid peroxidation, and increased inflammatory responses. Adapted from Mazzone et al, 2010.

The lungs are directly exposed to ambient air at large volumes from normal respiration and as so, it is exposed to exogenous oxidants. Internal sources of OxS may come from native lung cells.[12] These are often tightly regulated by sophisticated enzymatic and nonenzymatic antioxidant systems.[19] Among the consequences of OxS from CS are direct damages to DNA, RNA, amino acids, lipids, and an imbalance of oxidants to antioxidants(Fig.3).[20] However, the alteration of the cellular redox state, caused by CS, in the lungs can further enhance the production of ROS and worsen the burden of oxidate stress throughout the body.[19] Carcinogens within CS can also have marked effects on oxidative stress. Molecules such as NNK and NNN have been shown to affect the redox state of the cell during malignant transformation in different types of cells including endothelial and endothelial cells.[21, 22]

Incidentally, CS has also been linked to cardiovascular diseases (CVD) and it accounts for nearly 20% of all deaths from CVD per year.[12, 23, 24] CS can influence other risk factors related to CVD including glucose, insulin, and cholesterol levels.[12] However, CS can independently and synergistically increase the risk of CVD even when adjusting for other comorbidities.[11] Given that the cardiovascular and respiratory systems are so closely intertwined, it naturally follows that disruption of one affects the other. One noteworthy pathway that is disrupted in these two systems is the cellular redox state. Particularly, the endothelium of the vessels seems to show distinct effects when exposed to CS by disrupting the endothelial nitric oxide synthase (ENOS) pathway.[25] This pathway is intimately involved with OxS as superoxide, an oxidant byproduct of mitochondrial respiration, reacts with nitric oxide (NO) to form peroxynitre anions, another type of oxidant.[26, 27] Additional groups of molecules that are commonly found in CS are N-nitrosamines. These have been found to increase levels of markers commonly used for the detection of CVD including lipid peroxidation and OxS markers.[28] As previously discussed, (Fig.3), OxS can have a profound impact on cellular function. These events can form a cascade of damage that can explain the multi-organ effects seen in CS usage.

OxS has been established as one of the major pathways of insult caused by CS. The diversity of chemicals in CS brings about a varied selection of potential pathways to cause oxidative stress. Moreover,

it plays a major role in various diseases such as lung cancer, chronic obstructive pulmonary disease (COPD), and atherosclerosis. In addition to increased oxidative stress, CS can also deter the antioxidant defense system leading to a significant unbalance. Furthermore, recent works have shown that even in nicotine products with simpler compositions, such as e-cigs, OxS can have similar effects.[29-31]

1.3 Effects of Cigarette Smoke on the Brain

1.3.1 Introduction to Cigarette Smoke in the Brain

Undoubtedly CS has effects on the CNS as the only reason for tobacco consumption is the effects induced by nicotine. These include a slight feeling of euphoria, relaxation, and feeling of satisfaction that are caused mostly by nicotine's ability to bind and activate nAChRs in the mesolimbic area, the corpus striatum, and the frontal cortex among other areas.[49] The chances of becoming addicted to CS after a single use are as high as 32% making it more than other highly addictive drugs such as heroin (23%), cocaine (17%), and alcohol (15%).[49-51] Moreover, CS has been associated with neurological diseases both in epidemiologically and mechanistic studies.[10, 49, 52, 53] Studies indicate that smoking can assist in the generation of ROS, subsequently aiding in the progression of the BBB impairment by sustained inflammatory activity[3, 9]. It is also known that dysfunction of the BBB is present in individuals suffering from neurodegenerative disorders, such as Alzheimer's disease and other types of dementia[6]. Additionally, microglia have been shown to play an important part in the progression of neurodegeneration through sustained signaling of inflammatory factors[54]. Recent mounting evidence has shown that microglia activation leads to the production of amyloid β (Aβ), tau pathology, neuroinflammation, and reduction of normal neuronal function[55, 56].

1.3.2 Effects of CS and NNK on the Brain

CS contains a rich and diverse amount of chemicals, including N-nitrosamines and nicotine among others.[12] N-nitrosamines such as NNK are among the most potent carcinogen in CS. Nicotine can undergo

nitrosation within the cell, at the tobacco plant, with tobacco combustion or interact with ambient nitrogen to be converted into NNK and NNN which can then form DNA adducts and promote genetic damage and mutations (Fig.2).[15, 32] NNK can also metabolize into NNAL, another strong oncogenic chemical found in CS which itself have several oncogenic and bioactive forms (Fig. 4).[33-35] When NNK reacts with DNA it can form 7-*N*-methylguanine (7-mGua) and O^6-methylguanine (O6-mGua) as well as small amounts of O^4-methylthymine (O4-mTh) (Fig.2).[15] The mutagenic capacity of these varies with O^6-mGua showing high mutagenic activity when compared to other forms.[36] This is due in part to the low efficiency of the DNA repair mechanism when dealing with O^6-mGua as opposed to 7-mGua and O4-mTh .[37]

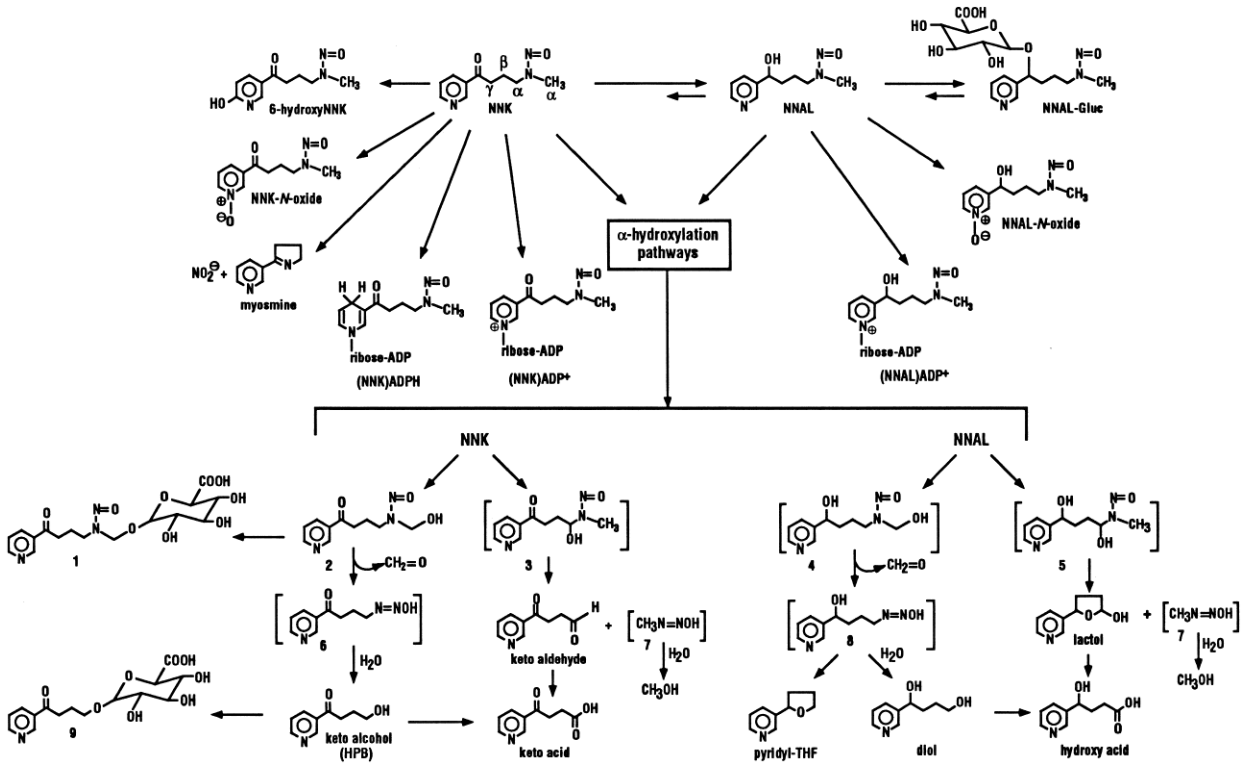

297

298 Figure 4: NNK metabolism pathways. Adapted from Hecht 1998.[33]

299

However, the effects of NNK are not limited to adduct formation. As previously mentioned, NNK has been found to be able to bind and activate nAChRs promoting cellular pathways including metabolic pathways.[38, 39] CS consumption typically promotes an increase in α7 homomeric nicotinic acetylcholine receptors (α7nAChRs) which have been shown to promote tumor growth but have also been implicated in cardiovascular disease and immune function.[40, 41] The brain presents a particularly vulnerable target due to the wide distribution of nAChRs, primarily α7nAChRs (Fig.5).[42] NNK has also been shown to decrease levels of gamma-amino butyric acid (GABA) while it's regulated by α4β2nAChR, which is desensitized in smokers.[15, 43] This presents an issue as α4β2nAChR regulates inhibitory actions that can potentially hamper deleterious effects of NNK activation of α7nAChRs.[44] Moreover, NNK has been linked to OxS directly by the creation of 8-hydroxy-2'-deoxyguanosine (8-OHdG) adducts, a lesion generated from ROS that is used as a marker of DNA oxidative damage.[45] Although the mechanisms of NNK-induced OxS are not well understood, it is evident that it can play a role in the detrimental effects seen with this molecule. Thus, the upregulation of α7nAChRs, desensitization of α4β2nAChR, lowers levels of GABA and direct increase of OxS offer an attractive explanation for the effects seen in NNK exposure.

315

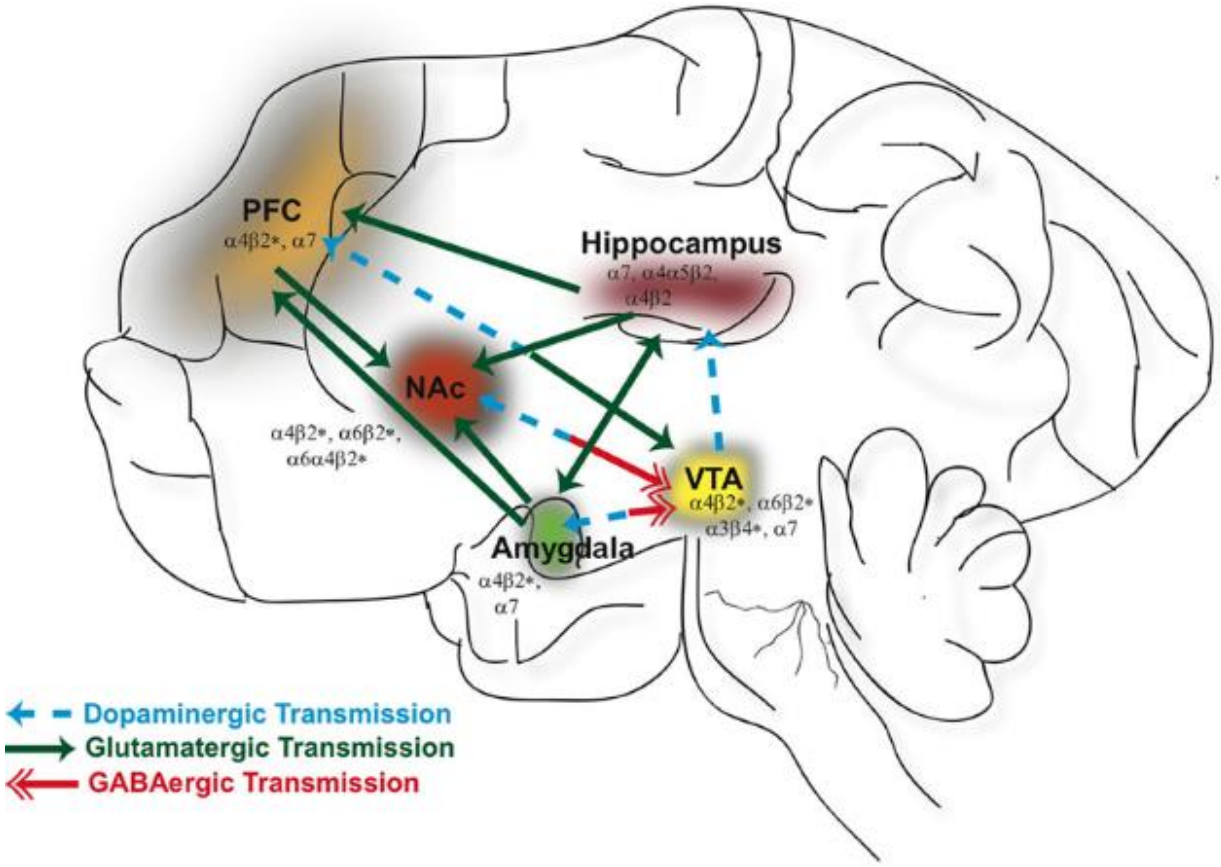

316

317 Figure 5: nAChRs are distributed in multiple regions of the brain. Adapted from Feduccia et al. 2012.[42]

318

NNK is among some of the strongest carcinogens found in CS with well-established literature addressing mechanisms of action in lung pathology.[46] These include the formation of DNA adducts and DNA oxidation which leads to aberrant cell function.[45-47] NNK has, as well, been found to be able to bind and activate nAChRs and promote cellular pathways including metabolic pathways.[38, 39] Studies have also shown that NNK has immunomodulatory effects in alveolar macrophages, a member of the mononuclear phagocyte system of which microglia are a part of.[48] The combination of these mechanisms can increase activity in cells with damaged DNA promoting further OxS to create an optimal microenvironment for aberrant cell function.

1.4 Key Players in Brain Homeostasis

1.4.1 Microglia

Microglia play an essential role in proper neuronal function as the resident macrophage cells in the CNS, which are accountable for the quick response to pathogens and other infiltrates[6]. Chronic activation and enhanced proliferation of microglia can contribute to sustained release of inflammatory factors, leading to reciprocal effects like BBB breakdown[54]. Morphological changes in response to insult have been a classical method for detecting a shift from homeostatic function to "activated" microglia (Fig. 6). However, there is limited knowledge about the molecular changes that accompany morphology change.[57, 58] Similarly to macrophages in the rest of the body, microglia operate in a manner that can be destructive to surrounding tissue upon the detection of insult.[59] Is it, therefore, that the activation of microglia must be tightly controlled as over-reactive microglia can cause unnecessary damage, but under-reactive microglia can result in dysfunction of other cells.[57]

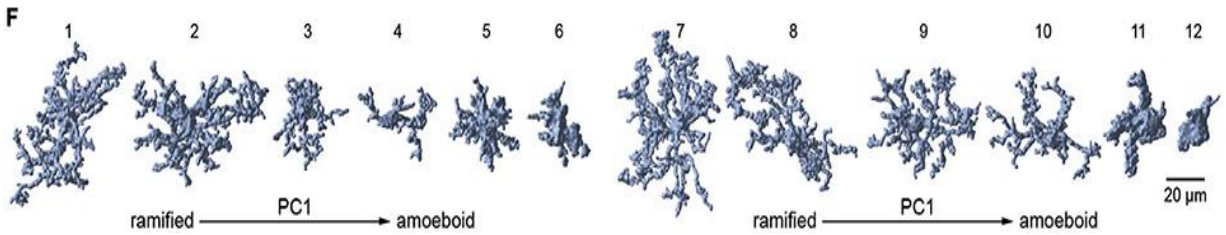

Figure 6: 3D reconstruction of different microglia morphological states in the cortex. Adapted from Heindl et al. 2018.[60]

Under normal conditions microglia dynamically respond to events such as synaptic pruning, clearing dead and surplus cells while remaining "inactivated" .[61] Using morphological changes, studies have been able to establish the surveying neighborhood of microglia to be about 10 times its cell body size.[62] It was believed that microglia soma remained static and that its projections performed and received all the changes.[63, 64] However, recent evidence has pointed to a more dynamic involvement of the microglia soma in both surveying and pathological conditions.[60, 65-67] Microglia can also have temporal and spatial heterogenicity. Changes of function over time are apparent in both neuronal development (e.g., fetal to juvenile to adulthood, etc..) and homeostatic function; while recent evidence has pointed to differences between microglia residing in different brain regions, such as the cortex, hippocampus, and cerebellum, displaying distinct glial makeup.[68, 69] During insult, microglia have been shown to mediate synaptic phagocytosis, response to chemical signaling, induce an inflammatory response, and mediate myelination (Fig. 6).[70]

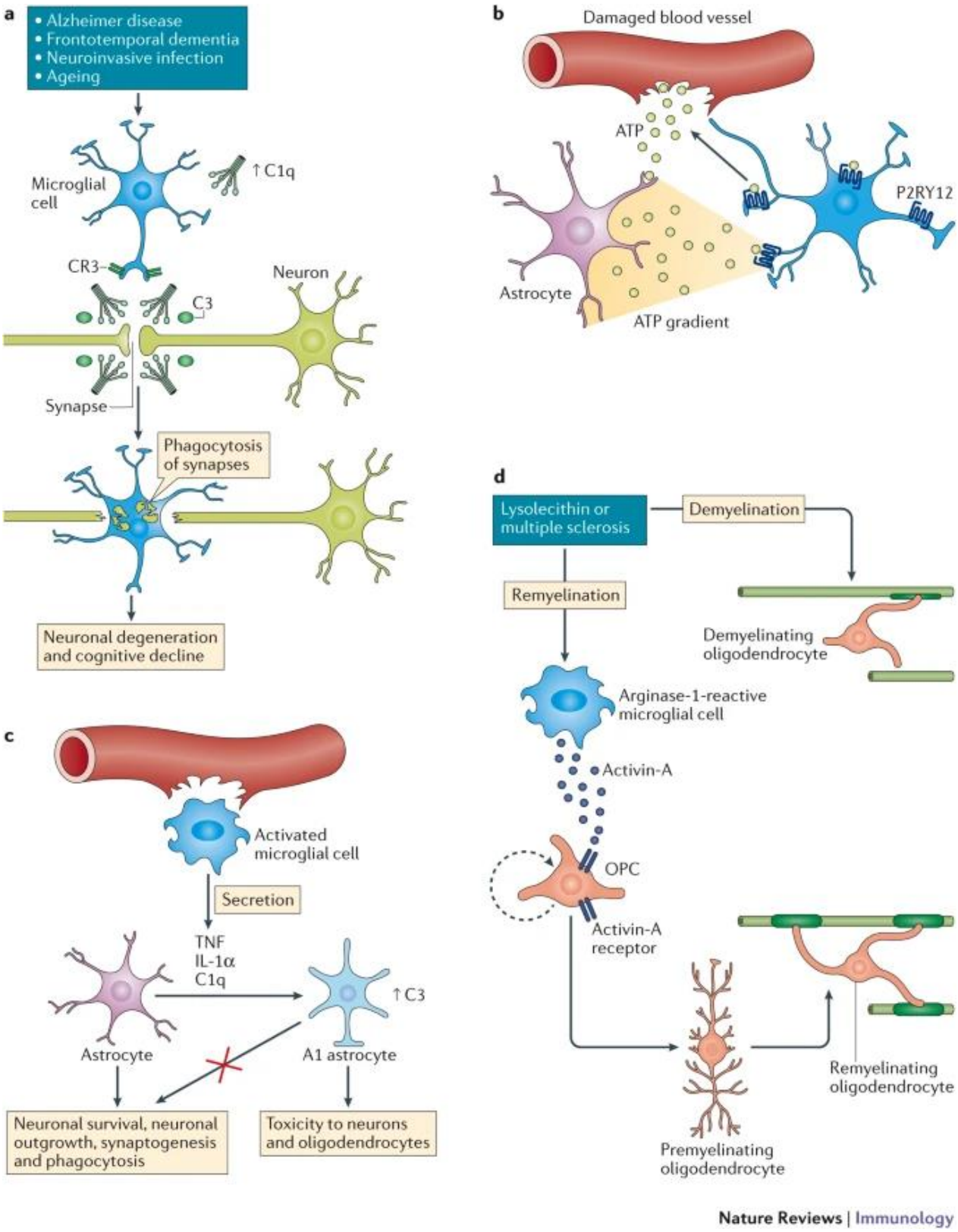
a
• Alzheimer disease
• Frontotemporal dementia
• Neuroinvasive infection
• Ageing
Microglial cell
↑C1q
CR3
C3
Neuron
Synapse
Phagocytosis of synapses
Neuronal degeneration and cognitive decline
b
Damaged blood vessel
ATP
P2RY12
Astrocyte
ATP gradient
c
Activated microglial cell
Secretion
TNF
IL-1α
C1q
↑C3
Astrocyte
A1 astrocyte
Neuronal survival, neuronal outgrowth, synaptogenesis and phagocytosis
Toxicity to neurons and oligodendrocytes
d
Lysolecithin or multiple sclerosis
Demyelination
Remyelination
Demyelinating oligodendrocyte
Arginase-1-reactive microglial cell
Activin-A
OPC
Activin-A receptor
Remyelinating oligodendrocyte
Premyelinating oligodendrocyte
Nature Reviews | Immunology

358

Figure 7:[70] Microglia function during insult. A) Synaptic loss and phagocytosis are mediated by microglia during normal function. B) microglia respond to tissue signaling molecules during injury allowing for movement towards the affected area. C) Local inflammation and microglia-mediated inflammation trigger the release of inflammatory cytokines inducing astrocyte reaction. D) Microglia mediated demyelination and remyelination in response to aberrant myelination processes and insult. Adapted from Li & Barres. 2017.

Previous studies have shown that persistent microglia-mediated inflammation in the brain affects neuronal plasticity, impairs memory, and can drive tissue damage in neurodegenerative disorders. Microglia were shown to have distinct signatures in neuroinflammatory disorders that were also found in neurodegenerative disorders suggesting a common subset of microglia population shared between the two.[71] As previously mentioned, the effects of CS at the cellular level include genetic damage and increased oxidative stress, both of which have a profound and diverse impact throughout the body. The mechanisms creating these effects seemingly have a two-prong effect on the immune system by either exacerbation of pathogenic immune responses or attenuation of defensive immunity. These properties can create complex reactions resulting in different diseases such as CVD, cancer, and COPD among others.[72] In the brain, CS exposure can alter brain function in multiple manners including response to insult. Studies have shown that CS can lead to decrease levels of markers of activation in microglia.[73] However, others showed that while markers of activation in microglia remain low, morphological changes to an activated state do occur. Findings also point to a differential effect observed in different regions, namely the nucleus accumbens showing a proinflammatory state with elevated ROS levels while the caudate putamen showed no change.[74]

1.4.2 The Blood Brain Barrier

Due to its limited repair ability, the CNS must control any and every particle it comes in contact with. This is mainly achieved through the BBB. The BBB is a multicell construct consisting of endothelia cells, pericytes, capillary basement membrane, and astrocytes, in a structure called the neurovascular unit (Fig.7). Due to the heterogenicity and dynamic nature of neural tissue, the BBB must maintain a highly restricted environment and meet different regional demands.[75] One such example of the specialization of these components are the endothelial cells and their modified abilities to restrict the flow of molecules by the use of thigh junctions (TJ), limited presence of caveolae at the luminal surface, and a high number of mitochondria.[76] Interestingly, endothelial cells of the BBB also express drug-metabolizing enzymes such as P-450, an enzyme that has been implicated in procarcinogen conversion of CS compounds.[77] Endothelial cells share the basement membrane with pericytes and allow for the exchange of ions, metabolites, and

391 signaling molecules for coordination of function. Pericytes can also perform contractile functions to control
392 blood flow, perform phagocytic functions, and have been shown to have multipotent stem cell
393 capabilities.[75, 78] Moreover, the BBB is comprised of astrocytes and, as the most abundant cell in the CNS,
394 these play a major role in performing pH regulation, neurotransmitter uptake, maintenance of parenchymal
395 space, and neuron-to-vasculature signal transduction.[79] As is often the case with complex systems,
396 dysfunction of one component can impact others creating an unbalance in the intricate equilibrium.

397

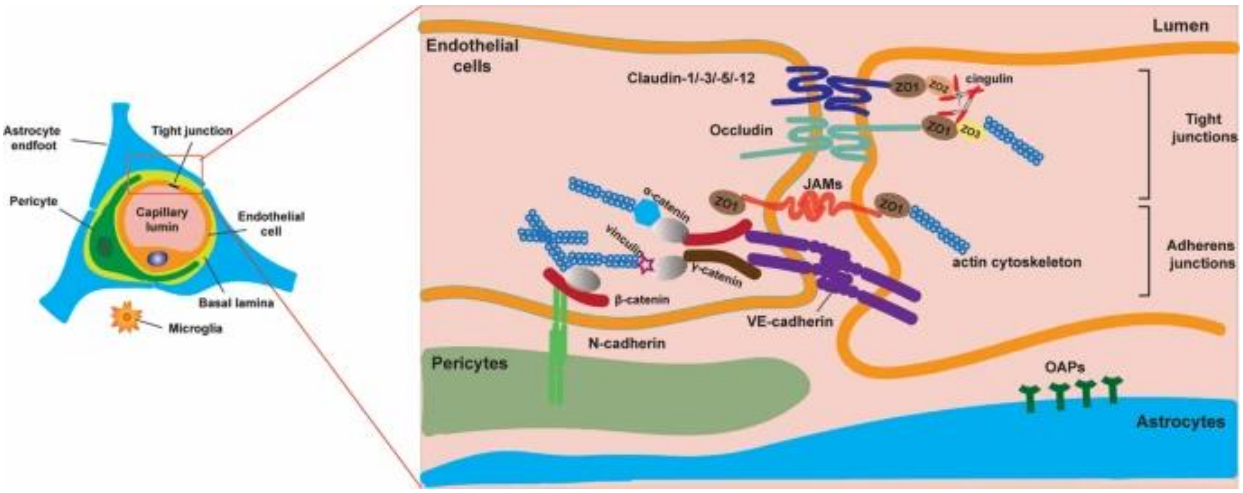

398

399 Figure 8: cells and constituents associated with the BBB. Adapted from Kadry et al. 2020.[75]

400

Notably, CS can affect one or more components of the BBB as it is the first point of contact of CS toxins in CNS exposure. Cell culture studies have shown that ROS can directly break down the BBB by TJ modification[80]. Due to the high content of ROS within CS, acceleration of TJ disruption occurs in the BBB[81]. Chronic exposure to CS has also been linked to small vessel ischemic disease (SVID), a disorder characterized by leaky micro-vessels in the brain leading to loss of BBB integrity and function. Hossain et al showed that CS decreases endothelia viability but not astrocytes or monocytes and at lower concentrations, CS showed increased pro-inflammatory cytokines.[81] Nicotine, and its metabolite cotinine, also play a role in BBB disruption. In an, *in vitro* BBB model of bovine brain microvessel, endothelial cells (BBMEC) treatment with nicotine and cotinine showed a decrease in zonula occludens-1 (ZO-1) that was mediated by alpha7 nAChR (Fig.8). [82] Nicotine has also been shown to disrupt the Na^+ K^+ $2Cl^-$ co-transporter which can introduce an unbalance in the BBB and potentially alter the response to normal and pathological conditions (Fig.8).[83] Nicotine and OxS can work synergistically to promote BBB dysfunction and potentially explain effects that have been observed in chronic CS users.[6, 84]

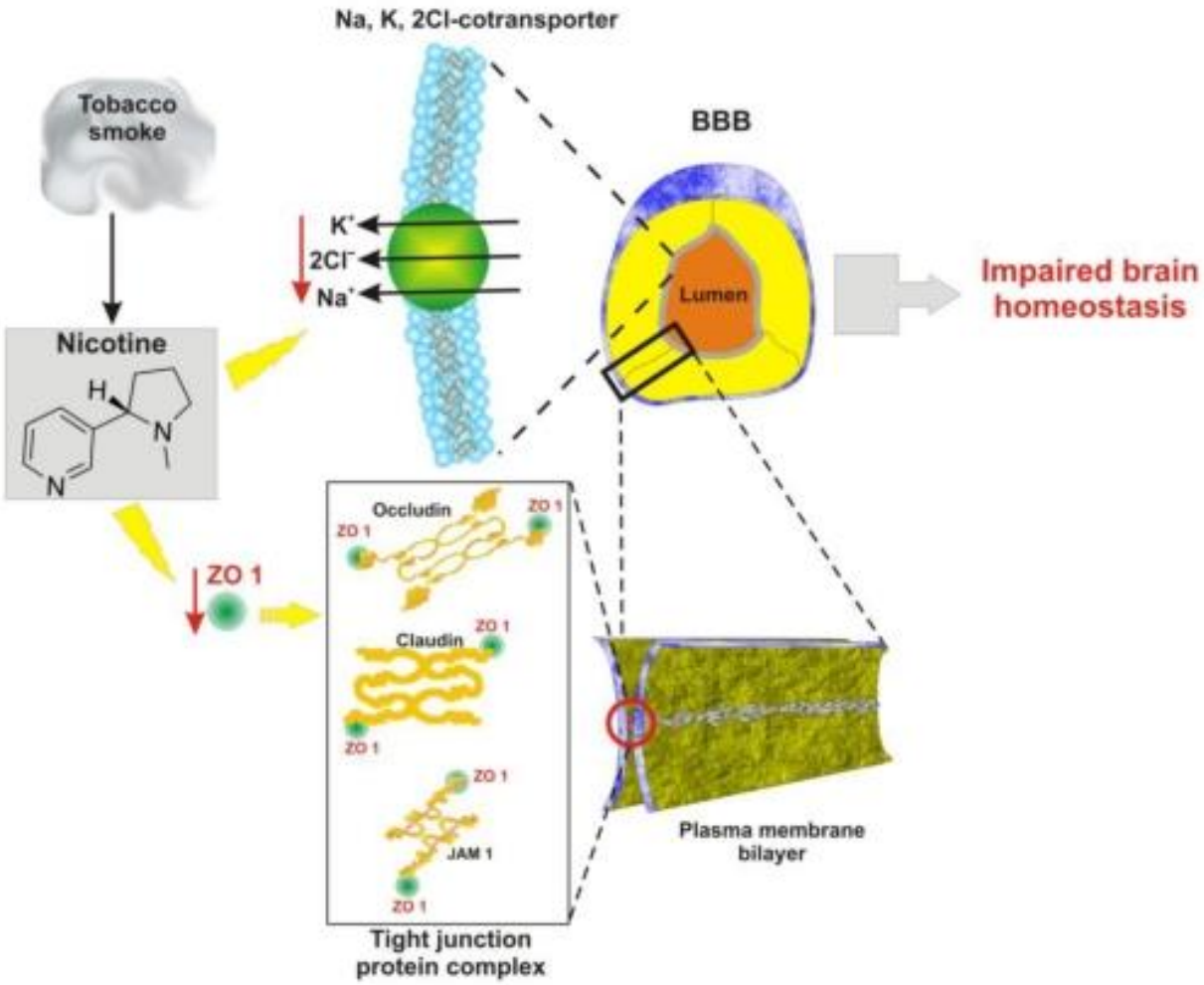

Figure 9:[6] Exposure to nicotine impairs BBB function. Nicotine decreases the expression of ZO-1, which is a critical component of a variety of tight junctional proteins and that of the Na, K, 2C co-transporter. This can lead to impaired BBB function and altered brain homeostasis. Adapted from Mazzone et al. 2010.

1.4.3 Oxidative Stress in the Brain

As previously mentioned, (section 1.2) CS has been consistently linked to oxidative stress. The persistent creation of OxS through CS exposure can have profound effects at the cellular and functional level.[6] OxS can also become self-propagating as it can induce cellular damage and inflammation and therefore creating further oxidative stress.[85] This combined with the brain's poor capacity to deal with OxS can lead to deleterious effects in a cell population with limited regenerative capabilities. That is perhaps the reason why OxS and altered levels of antioxidants have been reported in multiple neurodegenerative disorders and psychiatric illnesses including AD, Parkinson's disease (PD), Huntington's disease, depression, anxiety disorders, schizophrenia, and autism spectrum disorders.[86]

Due to the heterogenicity of the brain, OxS can have region-specific levels of damage. Studies have noted that the hippocampus, amygdala, and prefrontal cortex are some of the regions that have a higher susceptibility to oxidative stress.[86, 87] These regions are known to have several roles including memory processing and formation. Most notably, the hippocampus plays a major role in learning and memory while it has been noted that this region is one of the most metabolically active regions of the brain with a preference for glycolysis, a metabolic pathway that is prone to oxidative stress, instead of other pathways like the pentose phosphate pathway (PPP) which have been shown to be partially protective against oxidative stress.[88-91] Regional differences in the brain offer an attractive potential explanation for why certain diseases might affect some regions more than others or how toxicants, such as those found in CS, can seem to "target" certain regions of the brain.

Increased OxS burden due to CS consumption coupled with OxS-prone regions in the brain can offer a possible path to explain the acceleration of pathology observed in neurodegenerative disorders in habitual smokers. These observations might also offer insight into the mechanisms involved in some of the cell-specific effects observed in CS users such as microglia activation and the endothelia of the BBB.

1.4.4 Cigarette Smoke and Alzheimer's Disease

AD is a neurodegenerative disorder that affects around 50 million people worldwide and it's expected to increase to 113 million within the next 30 years.[92] It is typically characterized by Aβ-containing plaques and tau-containing neurofibrillary tangles that gather in neural tissue and alter synaptic function creating the characteristic cognitive impairment seen in AD.[93] Typically, AD confers two types of changes including a positive lesion (accumulation of tangles and plaques) and negative lesion (loss of neural tissue).[93, 94] Senile plate formation occurs as Aβ is deposited extracellularly after proteolytic cleavage of amyloid precursor protein (APP) by β-secretase and γ-secretase. Neurofibrillary tangles are formed of hyperphosphorylated tau protein that accumulates within neurons and causes a loss of cytoskeletal microtubules and tubulin-associated proteins.[93] Loss of neurons is seen in advanced cases of AD; however, initial events of synaptic loss can be seen at earlier time points where the loss of dendritic spines, pre-synaptic terminals, and axonal dystrophy occur.[95] AD can have multiple factors that increase the risk of development. Most notably these include age, genetics, metabolic diseases (diabetes and vascular diseases), and toxicant exposure through environmental factors or lifestyle (such as CS exposure from first, second, and third-hand smoke) among others (Fig.4).

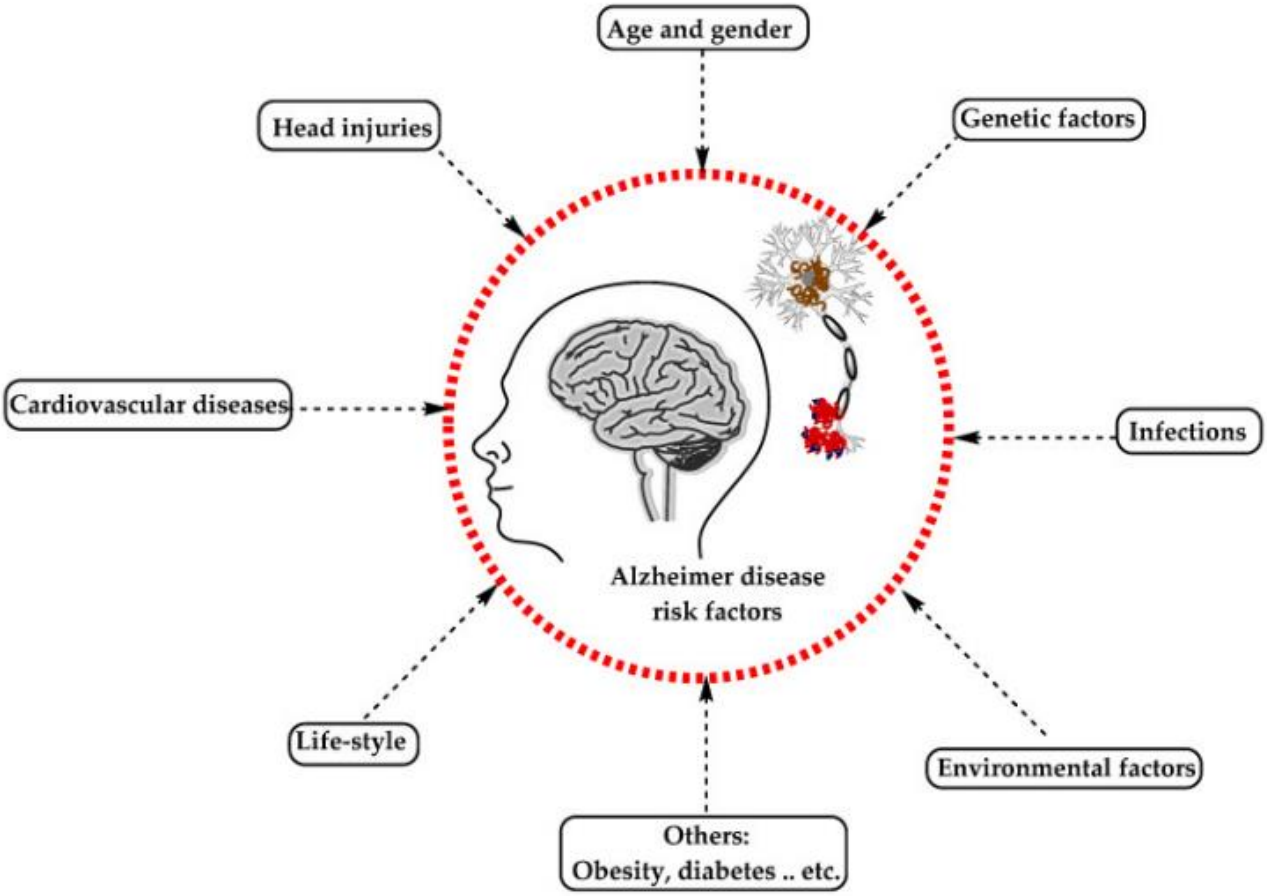

Figure 10:[93] Risk factors affecting AD. Adapted from Breijyeh & Karaman 2020.

Multiple mechanisms have been linked to the progression of AD and as a potential risk for its' development. Mainly, increase in OxS, DNA adduct formation, altered metabolic state, and vascular function disruption.[53, 93, 94] These have also been linked to worsening of risk factors linked to AD such as increased rate of infection, decrease capacity for injury repair, metabolic syndrome and CVD.[12] The collective body of research addressing CS as a risk factor for AD has been gaining momentum especially since the tobacco industry and affiliates stopped funding research into the matter.[53, 96] The studies strongly indicate that a history of smoking, whether it is a former or active smoker, is a significant risk factor that falls under the modifiable criteria. CS is not only associated with earlier onset of AD but also a reduction of lifespan of an average of 10 years [53] This can potentially create a survival bias in studies as the number of elder smokers is reduced in these studies due to premature death. Moreover, studies have found that other morbidities associated with CS, like CVD, cancer, and COPD among others, may limit the inclusion criteria and augment biases.[97]

1.5 The role of Intravital neuroimaging in studies of the brain

When investigating an organism, one is presented with a choice of approaches. Classically, probing of biological phenomena was done by taking a snapshot in time and conducting a forensic analysis on the extracted sample. As it can be expected, all dynamic information is lost, and one must piece together a picture from bits of information. To overcome these obstacles investigators have developed *in vivo* imaging that can capture aspects that cannot be seen in biopsies or models. Intravital microscopy (IVM) was developed to probe biological systems *in vivo* and in real-time by incorporating advance microscopy modalities. These take advantage of tissue optics, fluorescent properties of labeling molecules, and innate signals to visualize an event in a state close to its native form.

More commonly, IVM is done through confocal or multi-photon microscopy. Confocal microscopy uses a shallow depth of field, elimination of out-of-focus light through a pin hole, and the ability to image distinct optical sections from samples. This type of microscopy also takes advantage of the use of different wavelength lasers to illuminate the sample and distinguish between different targets.[98] These features offer

great advantages for IVM, but confocal microscopy is limited by the depth of penetration of light due to the use of shorter wavelengths. Another modality available for IVM is multi-photon microscopy (e.g., 2-photon microscopy). This modality uses similar concepts to confocal but differs in the wavelength of excitation, type of physical property to create fluorescence, no need for a pin hole, and increased depth of penetration of the light. The increased depth of penetration (~300μm) is due to the use of longer wavelengths in the near-infrared range coming from a titanium-sapphire (Ti:sapphire) laser that emits at 700 to 1100 nanometers. This type of laser differs from others as it is able to be tuned to the desired wavelength, offering great versatility. Moreover, because 2-photon microscopy can highly focus the area of excitation, it also provides a less phototoxic environment that is present in other modalities.[98] An additional advantage in 2-photon microscopy is the ability to use second harmonic generation (SHG). SHG is a second-order non-linear optical process in which two photons interact with non-linear optical media and combine to form a new photon with twice the frequency and half the wavelength of the initial photons.[99] This added advantage of 2-photon microscopy is more often used to visualize collagen but has been recently used in combination with exogenous probes to perform *in vivo* imaging.[100] A comparison of these two methods and their application for IVM is shown in Fig. 11.

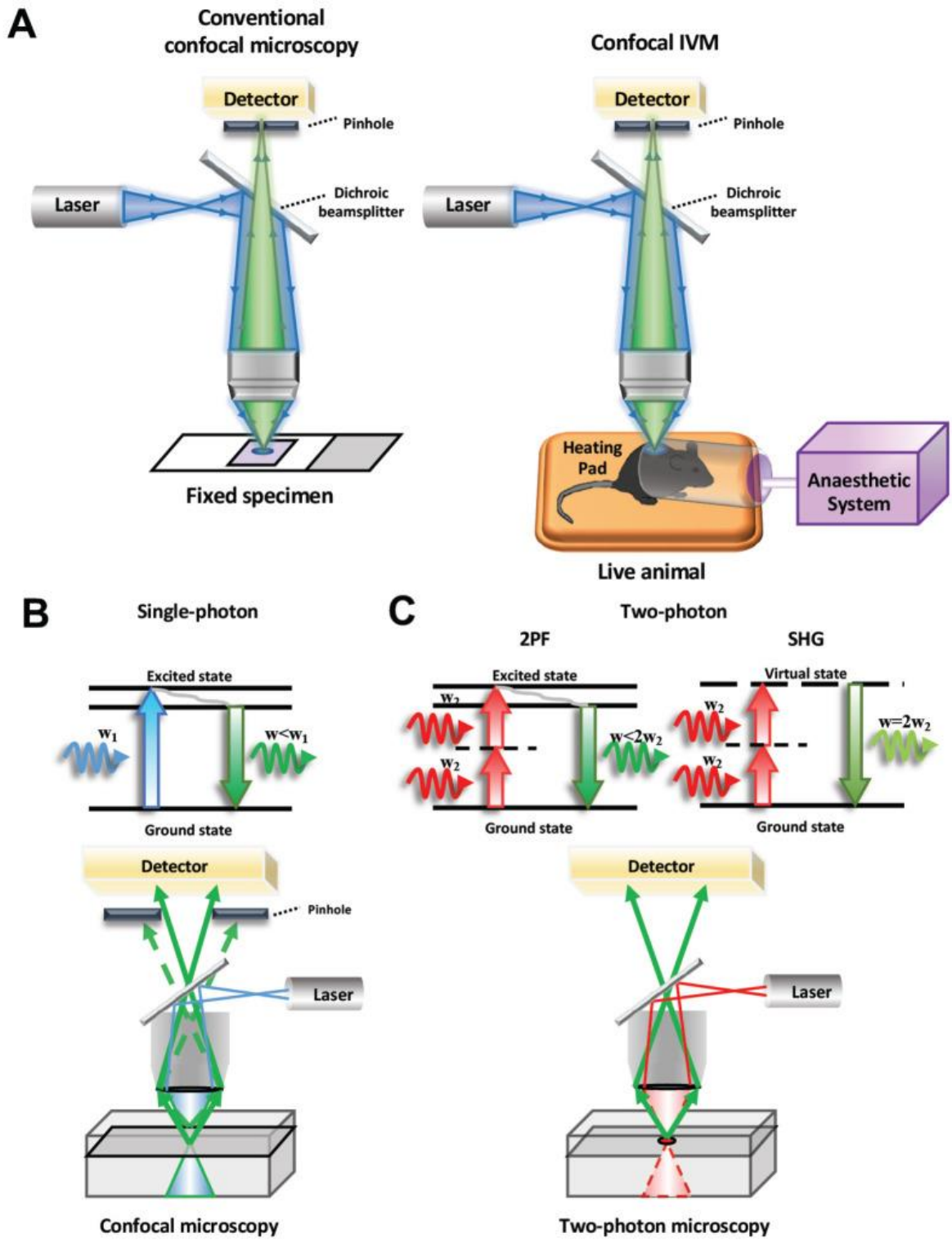

504

505 Figure 11: Comparison between conventional confocal microscopy with 2-photon microscopy in fixed and

506 IVM samples. Adapted from Choo et al. 2020.[101]

One of the most striking uses of IVM is in skull cranial window. Given the anatomy of the brain with its multiple layers of protection, it has been difficult to observe the brain in high detail. The field was limited by the use of magnetic resonance imaging (MRI) and positron emission tomography (PET) which offer a low resolution.[101] To address this issue one can use techniques such as cranial window and take advantage of the high-resolution microscopy offers. These typically come in the form of an open skull or thinned skull cranial window. In an open skull cranial window, all 3 layers of bone are removed leaving the dura exposed. A coverslip will then be fixed to the skull to cover the window and seal it with dental cement or other types of adhesives. After ~2 weeks of rest, imaging can commence however inflammatory effects might still be present at this time. In a thinned skull cranial window drilling is done only to remove the top cortical bone and cancellous bone leaving behind the bottom layer of cortical bone which typically ranges <100μm depending on the skill of the performing surgeon (Fig. 12). This method offers the possibility to image the day of the procedure with minimal inflammatory effects seen from the surgery. In addition to the ability to image neuronal cells, this type of surgery also allows for imaging of cells in the meninges including fibroblasts, macrophages, vasculature, and neuronal stem cells.[102] Additionally, this window can also be sealed in a similar manner to open skull cranial window and return to the site at a later time point.[103, 104]

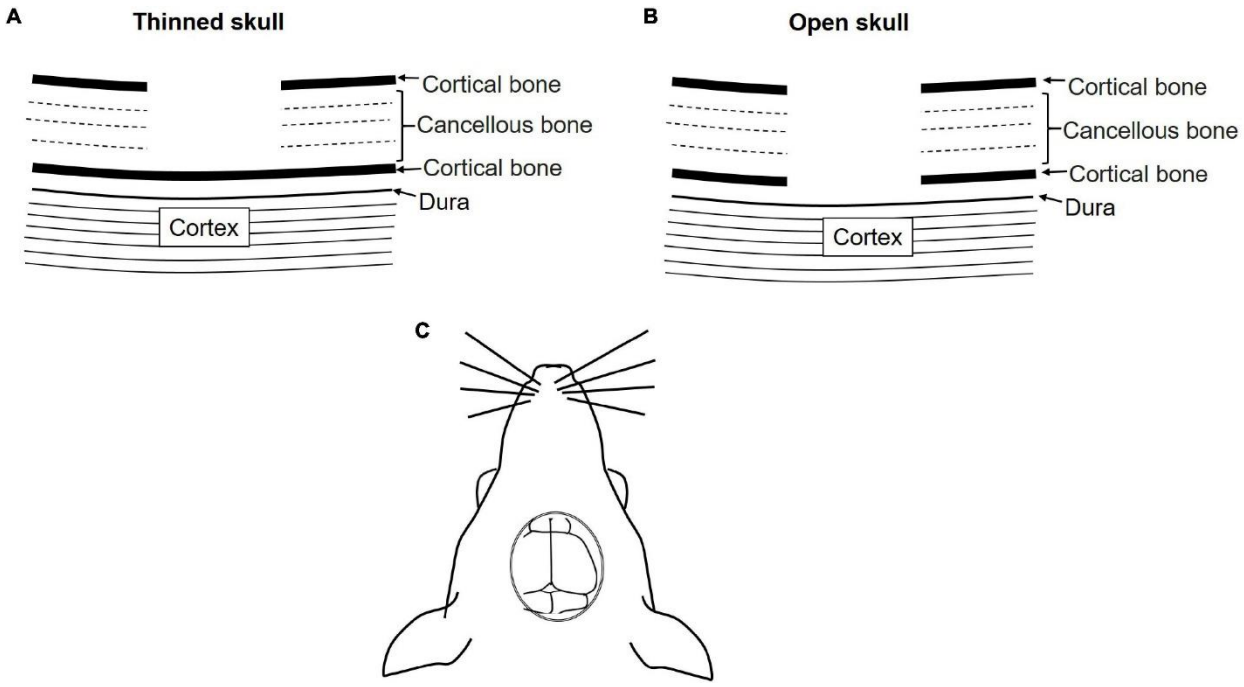

Figure 12: Comparison between open skull and thinned skull cranial window. Adapted from Vaghela et al. 2021.[103]

An often-forgotten aspect of IVM, and imaging in general, is data or image processing. With the power to capture a great amount of data comes the responsibility to manage and interpret the data. This aspect can be conveniently forgotten by many due to the seemingly foreign qualities that it involves. Qualities such as computing power, software handling and development, and digital image properties to name a few.[105] However, the meaning of data relies heavily on the ability of the researcher to understand the aspects involved. Separating information in an image can be done by applying different markers to different cells or cell components but morphometric qualities can also be used to separate features.[106] These often involve software that is either commercially available or custom-made.[107] Due to the nature of IVM using 2-photon microscopy, one often is limited by how many markers can be visualized at once. Using methods such as segmentation of features through image processing can help an investigator to find a deeper meaning in the captured data.

Chapter II: Aims of the Study

CS continues to be a leading cause of decline in quality of life as well as deaths globally. As a percentage of total population worldwide, smoking has seen a decrease since the 1980s, however, a surge in numbers of smokers is still seen due to an increase in population. It has long been known that CS is associated with complications in lung disease and cancer development but, more recently, it has been shown to have an association with neuroinflammation and other neurological disorders. Specifically, mounting evidence indicates a correlation /association between CS and AD. Studies indicate that smoking can aid in the generation of ROS and can impair the BBB by subsequent, sustained inflammatory activity. The mechanisms of this increase in inflammatory effects by CS, however, are poorly understood. While there is indication that CS induces neuroinflammation involving microglia and BBB breakdown, no focused effort has been taken to understand the role of BBB disruption and subsequent gliovascular responses. Further, NNK is a potent pro carcinogen synthesized from nicotine within the tobacco plant, from combustion, within the cell, and from interaction with ambient nitrogen that has been recently shown to have effects on the brain. One study revealed that intraperitoneal (IP) NNK treatment caused upregulation of proinflammatory markers in microglia and increased ROS stress. However, the route of delivery and dose given in this study do not necessarily reflect that of what is close to what a human might be exposed to. Among questions that remain are what the longitudinal effects of NNK on neuroinflammation and BBB integrity and what are the dynamic events involved. **Therefore, I hypothesize that NNK aggravates BBB breakdown and subsequently impairs microglial function.** To address the knowledge gaps in patterns of neuroinflammation induced by NNK in the whole brain, I propose to combine the use of transgenic mouse lines with IVM, whole organ optical clearing (OC), and large-scale microscopy. This approach has the potential to reveal a connection between inhaled toxicants, neuronal vulnerability, and progression of neurodegeneration through the use of a Cx3Cr1 transgenic mouse line (expressing GFP+ microglia) and advanced optical neuroimaging. The gap in knowledge of how NNK can potentially induce BBB as well as

glial abnormalities, which also may include dysfunction in gliovascular responses/interactions, may impact neuronal function and will be addressed through the following aims:

Specific Aim 1: To investigate the effects of NNK treatment on microglia using IVM and IF staining. I hypothesized that NNK treatment, whether it is acute or chronic, will induce a pro-inflammatory microglia response. Cx3Cr1 mice will be exposed to NNK in an acute (4 days) and chronic (18 weeks) timepoints with shams serving as controls. IVM will be performed to image microglia *in vivo* in 3D and in time. Analysis will be implemented to characterize the morphological changes of microglia by using ML segmentation of microglia soma. Findings will be confirmed with IF staining of extracted brains.

Specific Aim 2: To investigate patterns of BBB disruption caused by NNK treatment with IVM and real-time dynamics. I hypothesize that BBB breakdown will occur in animals treated with NNK and vascular changes will be visible through IVM. Cx3Cr1 mice will be exposed to NNK in an acute (4 days) and chronic (18 weeks) timepoints with shams serving as controls. *In vivo* changes will be tracked with IVM imaging, noting for BBB leakage and vasoconstriction and dilation. Brains will be extracted at select time points and sectioned, stained, and imaged for markers of BBB disruption as well as neuronal damage to corroborate *in vivo* findings.

Methods employed and studies associated with the aims are described as follows. Ch III will first describe methods developed and employed to address the aforementioned specific aims. In Ch IV the data acquired, and interpretation will be presented. CH V will present the conclusion and future direction of the work.

Chapter III: Methods

Intranasal Delivery of NNK

Animal experiments were performed according to the NIH Guide for Care and Use of Experimental Animals and approved by the University of Texas Medical Branch (UTMB) Institutional Animal Care and Use Committee (approval no. 1312058A). Male Cx3Cr1 mice (18 weeks old) purchased from The Jackson Laboratory (Bar Harbor, ME) were housed under pathogen-free conditions with food and water *ad libitum*. Mice were administered an intranasal dose of NNK or PBS serving as control. NNK (Sigma-Aldrich, N-076-1ML) was prepared at a concentration of 0.5 mg/kg in PBS. For intranasal delivery, mice were lightly anesthetized with 3% isoflurane for 1-2 minutes and 10 µl were delivered into each nostril with a 10 µl pipette (20 µl total). Mice were allowed to recover before placing back in the cage. This was performed 24 hours apart for 4 days and thinned-skull cranial window and imaging were performed on the 5th day. For chronic studies, Cx3Cr1 18 weeks old mice were administered NNK as previously mentioned for 5 days with two days rest for 12 weeks total and thinned-skull cranial window and imaging were performed 24 hours after the last dose. Because no previous known work had evaluated models with intranasal NNK, it was necessary to first test a range of doses. From literature we arrived at a common "low dose" (0.5-1.0 mg/kg-bw/day) and "high dose" (10-15 mg/kg-bw/day).[108-111] We then used the method of estimation established by Wei et al.[112] and applied a standard 10-fold inter-species and 10-fold intra-species uncertainty factors, along with a 10-fold chronic uncertainty factor to arrive at an average human daily dose exposure of 100 ng/kg-bw/day in a moderate smoker is roughly equivalent to the "low dose" estimate.

Thinned Skull Cranial Window and *in vivo* Microscopy

To visualize cortical vasculature a thin skull cranial window preparation was performed on anesthetized mice. To test the level of anesthesia, a toe pinch or tail pinch was performed prior to any procedures being performed. The head of the mouse was immobilized by using a stereotaxic device (Stereotaxic 520, Steoelting: Wood Dale, IL) and Ophthalmic ointment (NDC 11695-6832-1, Covetrus:

Dublin, OH) was applied to both eyes to prevent drying of the eyes during the procedure. The fur of the mouse was aseptically cleaned to prevent transmission of any microbes by wiping with 70% alcohol followed by sterile PBS. Fur was then removed using hair dilapidation (Nair: Ewing, NJ) and a midline incision was then made with the removal of fascia to expose the skull of the mouse. An imaging headpost ½ inch zinc flat washer (229489, Home Depot: Atlanta, GA) was then attached to the head of the mouse using cyanoacrylate (EM-02, Starbond: Los Angeles, CA)) to maintain PBS tension during imaging sessions. The cranial window procedure was performed inferior to bregma and parallel to the sagittal suture with a diameter of 5 mm. Using a high-speed hand drill (NC9010016, Braintree: Braintree, MA) with a round carbide bur, circular motions were made to remove the spongy bone. Fresh PBS and/or ACSF (597316, Harvard Apparatus: Holliston, MA), warmed in the incubator to prevent overheating of the skull, was continuously applied for the removal of bone dust, debris, and blood. The procedure was performed until the pial vessel was visible under a stereotactic microscopic (SMZ445, Nikon: Brighton, MI) and reached a depth in which the remaining skull thickness was approximately 20 microns. If bleeding occurred due to disruption of vessels within the spongy bone absorbable hemostat GELFOAM (09-0315-08, Pfizer: New York, NY) or bone wax (W31G, Ethicon: Cincinnati, OH) was applied until hemostasis ceased. Fresh PBS is then applied to the cranial window to ensure no bone dust or blood will impact imaging; the mouse is then placed under the microscope for visualization.

Intravital microscopy by multiphoton microscopy (MPM) was employed to visualize the cortex. MPM was performed utilizing an Ultima IV laser scanning nonlinear upright microscope (Bruker, Middleton, WI) with a Mai Tai (Spectra Physics, Santa Clara, CA) ultra-fast femtosecond laser as an illumination source tuned to 800 nm for fluorescence excitation. While on a heating pad the animal secured to the stereotactic device is placed on a custom-made stage under a 40X water immersion objective (NIR Apo, 0.80W, DIC N2, WD 3.5). Data taken from these studies include time series (T-series) and depth series (Z-series) for three-dimensional reconstructions. Approximately 6 sites were assessed per mouse, which includes T-series and Z-series. T-series acquired were taken with 1000 iterations with a 2.969 interval

and a frame size of 512x512. Z- series range in depth from 50-200 with a step size of 1.0 and frame size of 1024x1024. Fluorescence was collected using a 2-photon standard M filter set, with filter 1 parameters of bandwidth 604 ± 45nm, filter 2 parameters of bandwidth 525 ± 70nm, and a dichroic mirror cutoff at 575nm.

Ex vivo Brain Processing for Optical clearing: Delipidation

Mouse brains were processed following the SHIELD protocol.[113] Briefly, mice were transcardially perfused with ice-cold 1X PBS and then with SHIELD perfusion solution (10% (w/v) P3PE and 4% PFA (w/v) in 1X PBS) or ice-cold 4% PFA in PBS. Brain tissue was extracted and incubated in the SHIELD perfusion solution at 4 °C for 48 h and transferred to the SHIELD-OFF solution (1X PBS containing 10% (w/v) P3PE). After incubation at 4 °C for 24 h, the brains were placed in the SHIELD-ON solution (0.1 M sodium carbonate buffer at pH 10) and incubated at 37 °C for 24 h. Brains were then washed in 1X PBS at room temperature overnight and were cleared using stochastic electrotransport (SmartClear II Pro, LifeCanvas Technologies).

2-Photon Microscopy of Fixed Tissue

Fixed, CLARITY-processed sections (2 mm thickness, two-photon microscopy) were imaged using a Prairie Ultima IV (Prairie Technologies/Bruker, Middleton, WI) upright multiphoton microscope. For two-photon fluorescence microscopy, a 4X 0.16 N.A. air objective (UPLSAPO 4X, Olympus) and a 25X 1.05 N.A. super-objective (XLSLPLN25XGMP, Olympus) were used for image collection. Illumination for excitation of fluorescence was provided by a femtosecond laser (Mai Tai, Spectra Physics, Santa Clara, CA) tuned to 800 nm. Fluorescence was collected using a two-photon standard M filter set including filters with bandwidth 604 ± 45 nm, a filter with bandwidth 525 ± 70 nm, and a dichroic mirror cutoff at 575 nm. Samples were mounted on a 30-mm cage plate (CP06, ThorLabs, Newton, NJ) between two #1.5 cover glass.

Thin sagittal brain sections labeling

Brains were collected and fixed with 4% PFA at 4℃ overnight. Full brains were then hemisected and one hemisection was placed in 30% sucrose (S9378-1KG, Sigma-Aldrich, St. Louis, MO) on a shaker for 3 days. The hemisection was then placed in a tissue cassette (part number) and covered with OCT (237305771, Thermo Fisher, Waltham, MA) to be frozen. Cryosections of 30 µm were obtained using a cryostat (part number) and placed in a 12-well cell culture plate (part number) in PBS. Sections were washed with PBS and blocked/permeabilized with PBS containing 5% normal goat serum (part number) and 0.3% Triton-X-100 (part number) overnight at room temperature. After blocking, sections were stained with rabbit anti-Iba1 antibody (1:400, 019-19741, FUJIFILM Wako Chemicals, Richmond, VA), anti-CD11b, marker for resting microglia: Abcam ab133357 (rabbit:1:4000), anti-GFAP, marker for astrocyte: Agilent, Z033429-2 (rabbit:1:1000), anti-CD-68, marker for activated microglia: Abcam ab955(mouse:1;3000), anti-PSD95, synaptic marker for synapse damage: Thermo Fisher, MA1-045(mouse:1:500), anti-ZO-1, marker for tight junction: Cell Signaling Technology, 81933, (rabbit:1:1000). Anti-GFP: Thermo Fisher, A11122, (rabbit:1:2000), anti-Nrf2, marker for oxidative stress: Abcam, ab92946 (rabbit:1:1000), CDC25A polyclonal antibody, marker for DNA damage: Proteintech, 55031-1-AP, (rabbit:1:500) at room temperature overnight. Sections were washed and incubated with Alexa Fluor 647-conjugated goat anti-rabbit secondary antibody (1:400, Thermo Fisher Scientific, Waltham, MA) at room temperature overnight. At last, sections were mounted, and images were captured by confocal microscopy (LSM 800, Carl Zeiss Inc, Thornwood, NY).

Image Processing

Semi-automated microglia soma segmentation was done through a customized FIJI/ImageJ (v1.53) algorithm and with Waikato Environment for Knowledge Analysis [(WEKA) version 3.9.4] plugin. Image processing pipeline is as follows; dual channel raw images acquired from the 12-bit sensor were stored as 16-bit tiffs (a standard storage protocol that incorporates zero-padding of histogram values above 4095 (212-1) when using a 12-bit sensor). Images were contrast stretched to remove zero-padding prior to being converted to 8-bit images. Channels were split and the microglia channel was uploaded to WEKA plug-in.

Manual training was performed for the segmentation of microglia soma using and a subsequent step using a fast random forest algorithm was employed for machine learning automated segmentation. The yielding binary microglia soma mask was then used to create regions of interest (ROIs) and apply to the original microglia channel for microglia soma and ramifications extraction. The resulting two pseudo-channels were merged with the original 8bit image creating a five-channel image. For quantification, the five-channel images were uploaded to IMARIS (Bitplane USA, Concord MA) and 3D reconstructions were built. Minimum soma volume was calculated by sampling the smallest soma of 4 sham mice (30 somas per mice) and averaged to find a cut-off point. Analysis was done for the volume of somas, ramifications, Evans Blue within each component, and distance to vessels.

For stitching images, a zero-padding protocol was applied as previously mentioned to turn images into 8bit. A 2 × 2 median filter was applied to the image stacks. Stitching was performed with a 10% overlap of tiles having a field of view of 2327.3 × 2327.3 μm, providing 232.73 μm of co-registration in both X and Y coordinates. The Fourier Transform phase correlation stitching method was applied using the ImageJ plugin Grid/Collection Stitching.[115]

Statistical Analysis

Statistical analysis was done in R studio (version 4.0.2). To show the frequency of microglia cell body volume, a histogram was made with interval bins of 100μm. To further probe the data distribution, we constructed a box plot for each pairwise comparison to display the five-number summary of the data set and overlayed all individual data points to demonstrate all values including outlying points. The five-number statistical summary (the box plot) describes the minimum, first quartile, median, third quantile, and maximum. The box plots show skewed (not normally distributed) data. We proceeded to log transform all continuous variables to see if normality was met. Shapiro-Wilk's test noted that, in all cases, there was a significant difference (p-value<0.05) between the log transformed data and normal distribution. This indicates that log transformation did not result in normally distributed data. Therefore, a Mann–Whitney U test used to assess whether the means of the two treatment groups were equal. In order to compare microglial

2D time series findings to previously published parameters of microglia in 2D data,[65] we created a categorical dummy variable from the area parameter. Microglia having an area less than or equal to 53 μm^2 was categorized as "Surveying" and microglia having an area greater than 53 μm^2 was categorized as "Activated". Similarly, we created another categorical dummy variable to analyze the spatial relationship between microglia and vasculature, as first described by Bowyer et al 2020.[116] Microglia somas were categorized into one of the 3 classifications according to their respective distance from the surrounding vessels: contact (<5μm), close to vessel (≥5 to < 30μm), and far (≥30μm). A chi-squared test of independence was used to analyze if there was a significant association between all categorical variables and treatment groups.[117] A corresponding association matrix was constructed to show the dependency between the categorical variables analyzed. The legend displays the color hues corresponding to positive and negative adjusted residual values which shows the magnitude of the association. A positive value in the legend indicates the event happened more times than expected by chance alone. A negative value in the legend indicates the event happen fewer times than by chance alone. Together this construct gives indication on the nature of dependency between the variables and shows the relative contribution of each event in the association matrix to the total chi-square score. A qualitative score to characterize vessel events was performed on time series data. For vasodilation and vasoconstriction, an initial diameter was drawn using the straight-line tool in ImageJ/FIJI and compared to a final diameter. When the initial diameter was larger than the final diameter, the event was labeled as vasoconstriction while when the final diameter was larger it was labeled as vasodilation. For microhemorrhage, events of vessel content spillage were recorded. These events were tabulated and recorded as percentages of each event separately or as any event on the site. Specifically, the formulas are:

$$\frac{A\ vascular\ event\ (vasodilation\ or\ vasoconstriction\ or\ microhemorrhage\ )}{total\ \#\ of\ sites} = \%\ of\ singular\ event \qquad (1)$$

$$\frac{any\ vascular\ event}{total\ \#\ of\ sites} = \%\ of\ any\ vascular\ event \quad (2)$$

For all statistical tests, a significance level of α=0.05 was used.

Chapter IV: Treatment with Nicotine-derived Nitrosamine Ketone (NNK) Causes Disruption of Blood Brain Barrier (BBB) and Microglia Activation on Mice

Introduction

It has been known that cigarette smoke (CS) is associated with complications in pregnancy, respiratory disease, and coronary heart disease.[1, 118] Recent studies have also shown an association between neuroinflammation and several neurological disorders[3-5]. CS is composed of up to 7000 chemicals, including, N-nitrosamines, polycyclic aromatic hydrocarbons (PAHs), and reactive oxygen species (ROS)[6], that quickly flux into the oral mucosa, the lining of the epithelial airway, and ultimately spreads into body tissues, such as the central nervous system (CNS), through blood circulation. These CS toxins can trigger inflammatory mediators, like cytokines and chemokines that could potentially lead to neuroinflammation[5, 7]. Recent studies have also indicated that chemicals, such as N-nitrosamines specifically lead to neuroinflammation with effects that could contribute to the development of neurodegenerative disorders, like Alzheimer's disease (AD)[9,14]. These chemicals can also be found in any nicotine-containing products, along with nicotine deposited in ambient from product usage.[32]

NNK is among some of the strongest carcinogens found in CS with well-established literature addressing mechanisms of action in lung pathology.[34, 35, 119] These include the formation of DNA adducts and DNA oxidation which leads to aberrant cell function.[46, 47] NNK has, as well, been found to be able to bind and activate nicotinic acetylcholine receptors (nAChRs) and promote cellular pathways including metabolic pathways.[38, 39] The combination of these mechanisms can increase activity in cells with damaged DNA promoting oxidative stress. Studies have also shown that NNK has immunomodulatory effects in alveolar macrophages, a member of the mononuclear phagocyte system of which microglia are a part of. [48]

While impaired inflammatory function has been well-documented in chronic smokers at a systemic level[118], it is intriguing that the effects of cigarette smoke on neuroinflammation[3, 4, 9, 73] and neuroinflammation mediated by microglia[109, 120] have recently been shown in mice. Microglia play an

important role in proper neuronal function as the resident macrophage cells in the CNS, which are accountable for the quick response to pathogens and other infiltrates[6]. Chronic activation and enhanced proliferation of microglia can contribute to sustained release of inflammatory factors, leading to reciprocal effects like blood-brain barrier (BBB) breakdown[54]. In one study, Ghosh et al., investigated the action of IP-delivered NNK on the brain and revealed through immunohistochemistry that resident microglia accompanied by neighboring neuronal damage occurred within days of injection[109].

Other toxicants, such as ROS, in CS have been found to affect neurodegeneration by eliciting dysfunction in the BBB[6, 81, 121]. The BBB restricts the traffic of molecules from circulating blood to the CNS by providing a selective system that dynamically responds to metabolic needs[122]. Disruption of this construct allows the infiltration of foreign objects which can prompt events leading to neurodegeneration[121]. Cell culture studies have shown that ROS can directly break down the BBB by tight junction (TJ) modification[80]. Due to the high content of ROS within CS, acceleration of TJ disruption occurs in the BBB[81]. It is noteworthy that NNK has been found to induce ROS production in cancer stem cells and if present in the circulation or brain could provide an added source of ROS stress and dysfunction of the BBB.[123]

In this study, we aimed to study the effects of acute (4 days) and chronic (12 weeks) intranasal NNK treatment on the BBB and microglia using *in vivo* two-photon imaging. NNK was delivered intranasally as a form of delivery that is closer to exposure in humans. We demonstrated that acute NNK treatment compromised the integrity of the BBB and caused microhemorrhages along with irregular vessel dilation/expansion. Effects were also observed in microglia seen as an increased number of microglia with ameboid morphology in both the overall field of view (FOV) and along blood vessels. These effects were sustained in chronic NNK treatment. Although NNK can freely cross the plasma membrane at relatively high concentrations (Jorquera et al), at the concentration used in this study, NNK can cause BBB disruption, creating microhemorrhages. These small brain hemorrhages can cause NNK to leak into neural tissue potentially causing microglia activation and neurodegeneration.

Results

Microglial Responses in Acute NNK Treatment

Previous studies have demonstrated that when mice were treated with NNK through an IP injection an upregulation of proinflammatory cytokines and increased ROS stress was seen in microglia and astrocytes.[109] We reasoned that in light of these events, microglia morphological changes could be observed with IVM. We hypothesized that for an acute treatment of NNK morphological changes of microglia towards an activated state (more ameboid than ramified) would be observed in the prefrontal cortex of mice under IVM. We, therefore, exposed CX3CR1 mice to NNK through intranasal delivery for 4 consecutive days. Preliminary intranasal delivery testing of NNK concentration was done to determine a working solution. From literature we arrived at a common range of exposure (0.5-15 mg/kg-bw/day) then used a standard 10-fold inter-species and 10-fold intra-species uncertainty factors, along with a 10-fold chronic uncertainty factor to arrive at an average human daily dose exposure of 100 ng/kg-bw/day in a habitual smoker is roughly equivalent to 0.5 mg/kg-bw/day.[108, 110-112] Imaging was performed on the 5th day in the thinned skull above the prefrontal cortex of the mouse brain and in-depth optical section, as well as time-lapse imaging was taken *in vivo*. Figure 1 shows representative 3D reconstructions of NNK and PBS groups that went through ML segmentation for somas (Fig. 13A, C. Size analysis based on 3D volumes was performed and a color representation of volume was created – in Fig 13 the heat map show vessels represented in grey and different volumes of somas represented in red-shifted colors as larger volumes while blue-shifted colors showed smaller volumes (Fig. 13B, D). A histogram analysis shows that the control group had the great majority of the somas in volumes of 300 μm^3 or less while a portion of soma volumes in NNK treated can be seen in the 500 μm^3 range or greater. This establishes a distinct shift in microglia soma volumes between groups (Fig. 13E). A Mann–Whitney U test showed a statistical significance between the two groups (n=3 per group, $p<4.794^{-9}$) while PBS shows the majority of the data point in smaller values with fewer outliers and NNK shows a robust distribution of data points with an increased number of outliers (Fig. 13F). Increased soma size has been used as a surrogate parameter for

activation in the literature [65] but prior work has been limited to 2D histological data. For comparison with such work, we analyzed soma sizes in 2D from our time-series acquisitions. Previous studies found that the average surveying microglia has a soma area of 53 μm^2 and activated microglia tend to fall above that value.[65] Using these measurements, we grouped microglia soma areas into two categories and found that up to 39% of microglia showed a large soma size, consistent with the morphology of activated microglia (Heindl et al. and Li Q), in NNK treated while PBS showed 31% (Fig. 14A). A corresponding association matrix was then created to show the relationship between the microglial state (activated or surveying) and the treatment groups (NNK or PBS). Briefly, a positive value in the legend indicates the event happened more times than expected by chance alone and a negative value in the legend indicates the event happen fewer times than by chance alone. The chi-squared test between microglial state and treatment groups gave a p-value = 0.0001485, indicating there is an association between the variables. The corresponding association matrix shows the dependency between the categorical variables analyzed (Fig. 14B). The event of acutely treated NNK + Activated has a positive adjusted residual value, indicating that there are more activated somas associated with NNK treatment than would be expected by chance alone. The event of acutely treated NNK + Surveying has a negatively adjusted residual value indicating that there are less activated somas associated with NNK treatment than would be expected by chance alone.

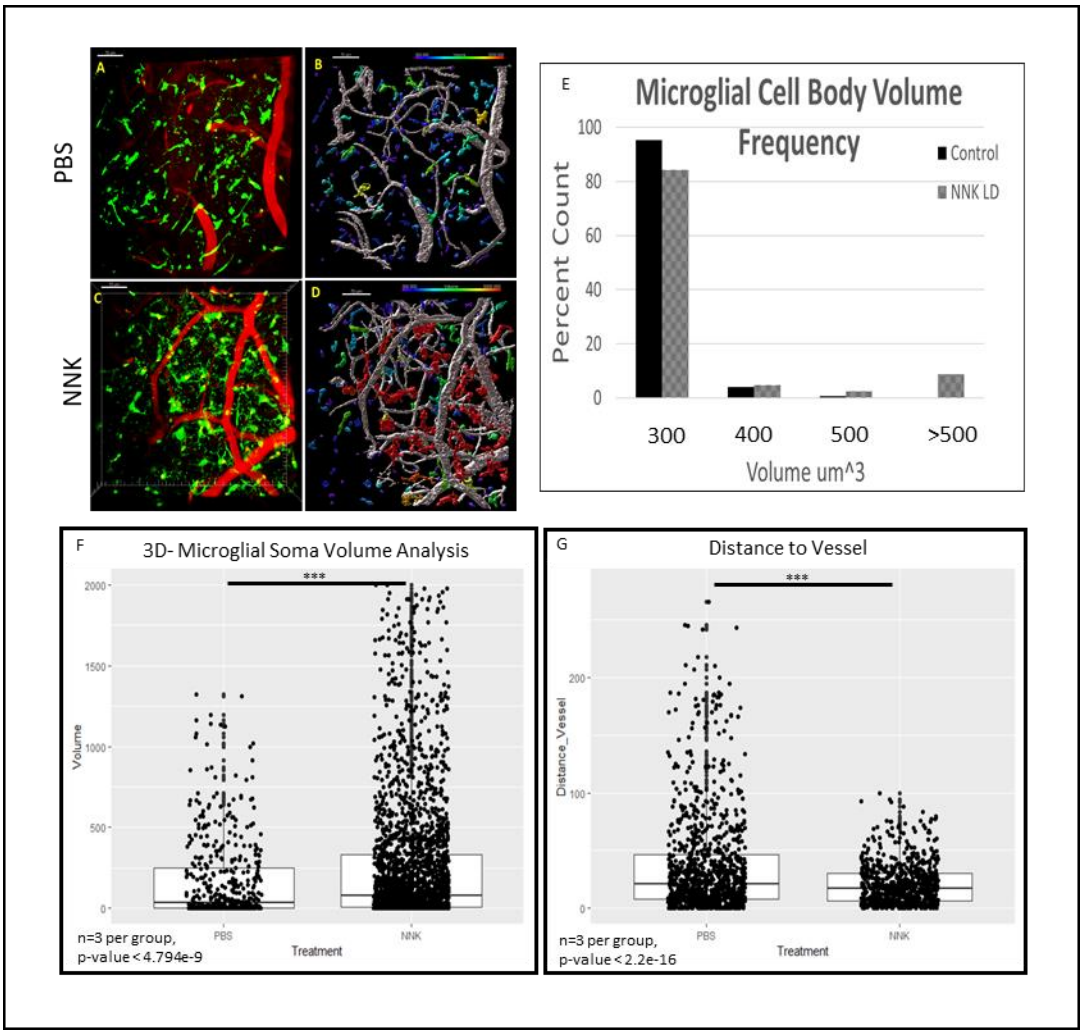

Figure 13: Microglia Soma changes with Acute NNK Treatment. A & C) IMARIS generated 3D reconstruction and ML learning segmentation of microglia soma (green) with vessels (red). B & D) IMARIS generated heatmap showing microglia soma arranged by volume. Blue shifted items represent smaller volumes and red-shifted items represent larger volumes. Vessels are shown in grey. E) histogram of microglia somas arranged by volumes in bins of 100µm^3. F) Box plot of microglia soma volumes in µm^3, *n=3*. G) Boxplot of microglia soma distance to vessel in µm, *n=3*. ***$p < 0.0001$, Mann–Whitney U test.

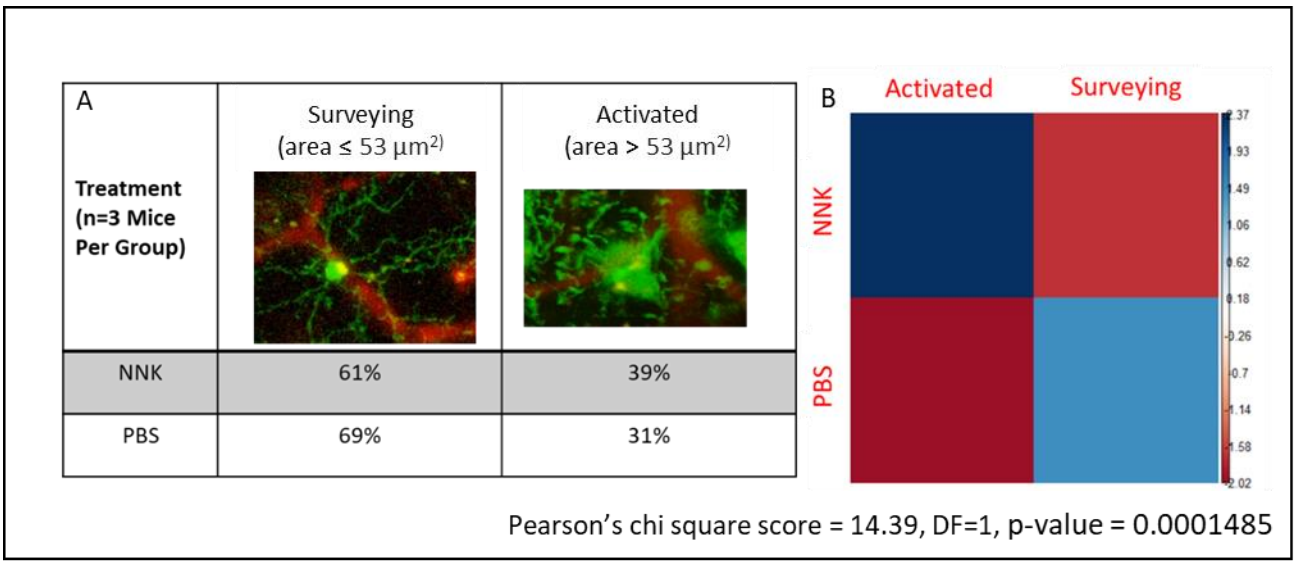

829

830 Figure 14: Classification and quantification of 2D microglia morphology. A) Classification of microglia
831 using soma area revealed an increased number of activated microglia in acutely treated NNK mice. B)
832 Matrix of association graphical representation of NNK vs PBS microglia morphological state. Data
833 demonstrates that NNK has a positive association with activated and a negative association with surveying
834 microglia. The opposite is true for the PBS group. Pearson's chi square score = 14.39, DF=1, p-value =
835 0.0001485.

836

Previous studies have identified microglia grouping on vessels as a response to pathology.[124] We, therefore, analyzed microglia somas for said behavior using distance (in μm) to vessel to determine the relative position of somas and noted the NNK group showed a statistically significant ($n=3$, $p<2.2^{-16}$) decrease in distance to vessels when compared to the PBS group (Fig. 13G). This shows that there is a noticeable grouping of microglia somas with vessels in the acutely treated NNK group. To further understand the relationship of soma proximity to vessels, we constructed an association matrix where we grouped somas into 3 classifications according to distance to vessels: contact (<5μm), close to vessel (≥5 to 30μm), and far (>30μm) (Fig.15). For this analysis, we used ML segmented somas (Fig.15A, C) and determined grouping through findings from previous studies.[116] The chi-squared test for independence between soma association to vessel and treatment groups gave a p-value = 2.828^{-9}, indicating there is an association between the variables (Fig. 15E). The event of acutely treated NNK + Contact and NNK + Close has a positive adjusted residual value, indicating that there are more somas in contact and close to vessels associated with NNK treatment than would be expected by chance alone. The event of acutely treated NNK + Far has a negatively adjusted residual value indicating that there are fewer somas far from vessels associated with NNK treatment. The event of acutely treated PBS + Contact and PBS + Close has a negative adjusted residual value, indicating that there are fewer somas in contact and close to vessels associated with PBS treatment. The event of acutely treated PBS + Far has a positive adjusted residual value indicating that there are more somas far from vessels associated with PBS.

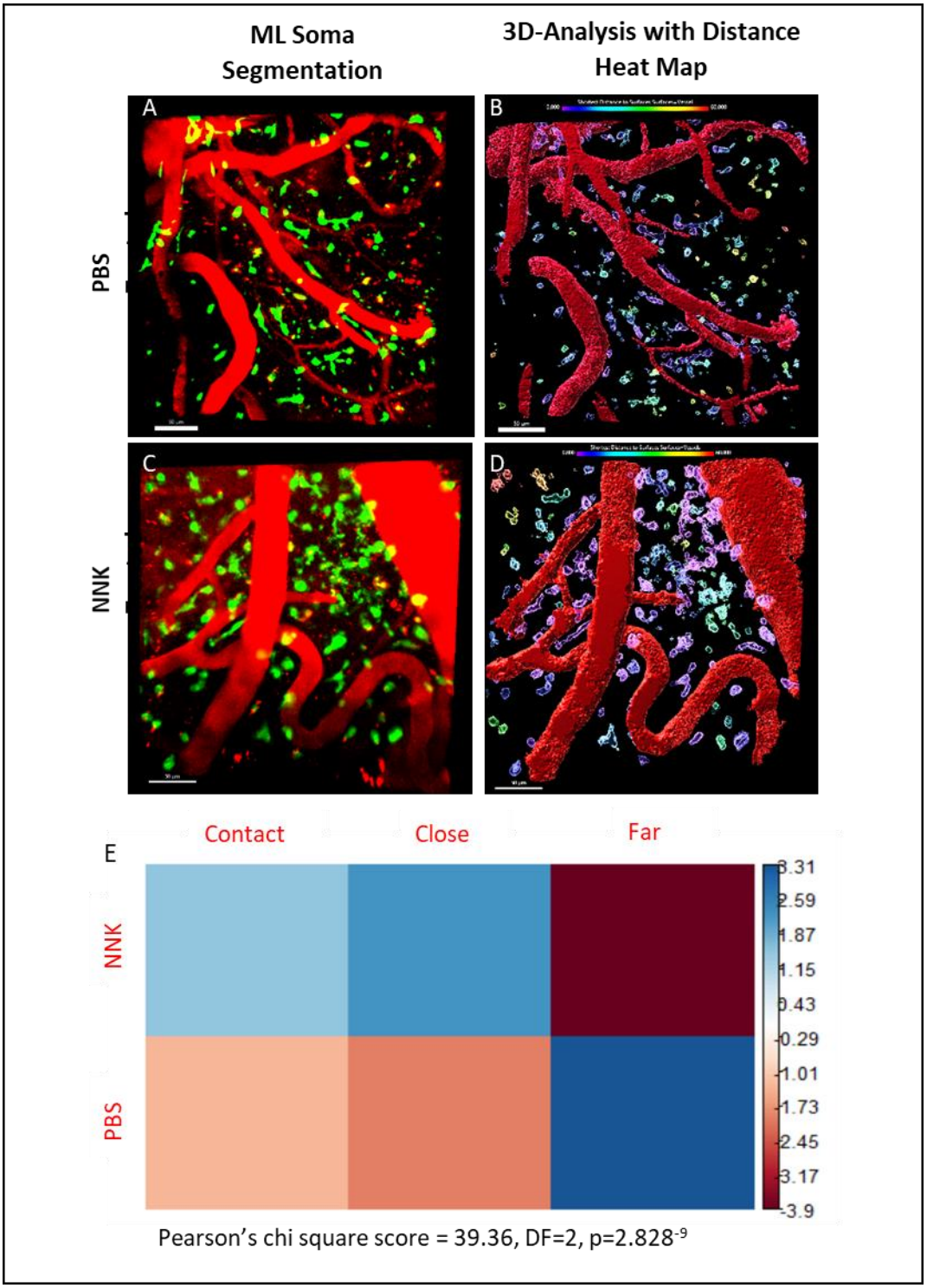

Figure 15: Association analysis of microglia soma and proximity to vessel. A&C) IMARIS generated 3D reconstruction of control and NNK z-stack with microglia bodies segmented using machine learning. Green is eGFP expressing microglia and red is Evans Blue labeled blood vessels. B&D) IMARIS generated color-

coded rendering of control z-stack with blue-shifted items representing somas closer to vessels and red-shifted items representing somas away from vessels. E) Matrix association analysis of microglia somata grouped into contact (<5μm), close to vessel (≥5 to 30μm), and far (>30μm). Acutely treated mice with NNK show a positive association with contact and close classification but a negative association with far. The opposite is true for PBS-treated mice. Pearson's chi square score = 39.36, DF=2, $p=2.828^{-9}$.

Microglial Responses in Chronic NNK Treatment

In a similar manner to acute treatment, Cx3Cr1 mice were treated with NNK for 12 weeks for the chronic portion of this study. To understand if the effects that were observed in the acute treatment of NNK are sustained after 12 weeks of treatment, we performed a correlation matrix of association analysis where we grouped somas into 3 classifications like that of Fig. 15E [contact (<5μm), close to vessel (≥5 to 30μm), and far (>30μm)] and noted that associations seen chronic treatment are similar to those in acute treatment. The chi-squared test for independence between soma association to vessel and treatment groups gave a p-value = 2.2^{-16}, indicating there is an association between the variables (Fig. 16A). The chronic NNK group shows a positive association with the contact classification and a negative association with far but shows a negative association with close classification. For the PBS group, we again see a negative association for contact classification and a positive association with close and far classification (Fig. 16A). These results show similarities with that of acute but differ in the close classification (Fig. 15E and Fig. 16A). Using previously mentioned measurements (Fig. 14A), we grouped microglia soma areas into two categories and found that up to 36% of microglia showed an, activated morphology in NNK treated while PBS showed 26% (Fig. 16B). In the 2D classification, we see the same pattern seen in acute with chronic NNK group positively associated with activated microglia and negatively associated with surveying microglia while the opposite is true for the chronic PBS group (Fig. 16C). When we analyzed microglia soma volume in chronically treated samples, we observed a similar distribution to that of acutely treated (Fig. 13F). The analysis showed a statistical significance between the two groups (n=3 per group, $p<2.2^{-16}$) while PBS shows the majority of the data point in smaller values with fewer outliers and NNK shows a robust distribution of data points with an increased number of outliers (Fig. 16D). Likewise, the analysis of distance to vessel showed similar trends to that of acutely treated (Fig. 16E), in which microglia have migrated to the vasculature and are in close contact in the NNK treated cases.

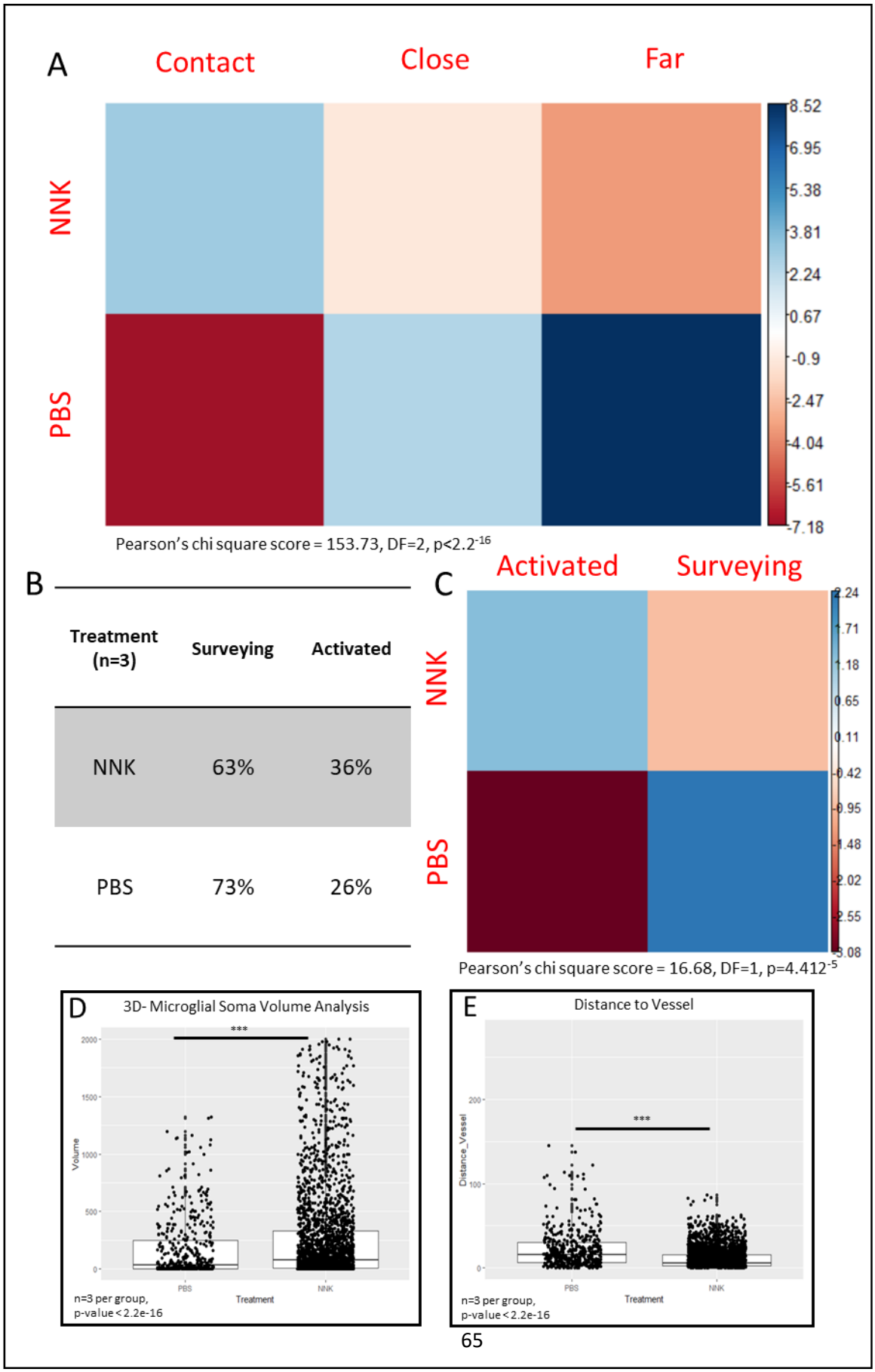
A
Contact
Close
Far
NNK
PBS
8.52
6.95
5.38
3.81
2.24
0.67
-0.9
-2.47
-4.04
-5.61
-7.18
Pearson's chi square score = 153.73, DF=2, p<2.2-16
B
Treatment (n=3)
Surveying
Activated
NNK
63%
36%
PBS
73%
26%
C
Activated
Surveying
NNK
PBS
2.24
1.71
1.18
0.65
0.11
-0.42
-0.95
-1.48
-2.02
-2.55
-3.08
Pearson's chi square score = 16.68, DF=1, p=4.412-5
D
3D- Microglial Soma Volume Analysis
***
Volume
2000
1500
1000
500
0
PBS
NNK
Treatment
n=3 per group,
p-value < 2.2e-16
E
Distance to Vessel
***
Distance_Vessel
200
100
0
PBS
NNK
Treatment
n=3 per group,
p-value < 2.2e-16

Figure 16: Effects of chronic NNK treatment on microglia somas. A) Matrix association analysis of microglia somata grouped into contact (<5µm), close to vessel (≥5 to 30µm), and far (>30µm). Chronically treated mice with NNK show a positive association with contact classification but a negative association with close and far. The opposite is true for PBS-treated mice. Pearson's chi square score = 153.73, DF=2, $p=2.2^{-16}$. B) Tabulation of microglia divided into two groups, surveying and activated. C) Matrix of association analysis of NNK vs PBS microglia morphological state. Data demonstrates that NNK has a positive association with activated and a negative association with surveying microglia. The opposite is true for the PBS group. Pearson's chi square score = 16.68, DF=1, $p=4.412^{-5}$. D) Box plot of microglia soma volumes in μm^3, *n=3.* E) Boxplot of microglia soma distance to vessel in µm, *n=3.* ***$p < 0.0001$, Mann–Whitney U test.

Vasculature Changes and Microhemorrhages Occur in Acutely NNK Treated Mice

By using IVM, we are able to observe dynamic vascular responses. Figure 17 highlights a time course event of a vessel appearing to be thinner (Fig.17A) and later expands to a thicker state, as with superimposed yellow lines (Fig. 17B). Briefly, yellow lines were added to various vessels at a later time point and then superimposed back to the initial time point to compare the changes in diameter. As noted above (Fig. 13-16), surrounding dynamic, microglia appear to be retracting their processes around vascular events, implying possible signaling for vasculature alteration. This direct contact is of interest for further investigation as some limited reports indicate microglia interaction with vessels can directly impact vessels responses such as leakage[54, 70], and vasospasms.[125] NNK exposed mice also revealed vessel integrity disruption seen as microhemorrhaging (Fig 17C). Another significant event noted in NNK-treated subjects was vasodilation (Fig. 17D). Like in other vascular events, vasodilation occurred near areas with microglia that appear to be adopting an ameboid morphology (Fig. 17 & 18). When the two groups were compared, a clear distinction in vascular events was apparent as the PBS group showed only events of vasodilation in 11% of the sites surveyed while the NNK group showed events of vasodilation in 42% of the sites, vasoconstriction in 26% of the sites and microhemorrhages in 47% of the sites (Fig. 17E). Some of the sites had multiple types of events with vasodilation and microhemorrhages being commonly found together. When we compared the total of any type of event happening in the FOV there was 11% total in PBS while NNK had 72% total (Fig. 17E).

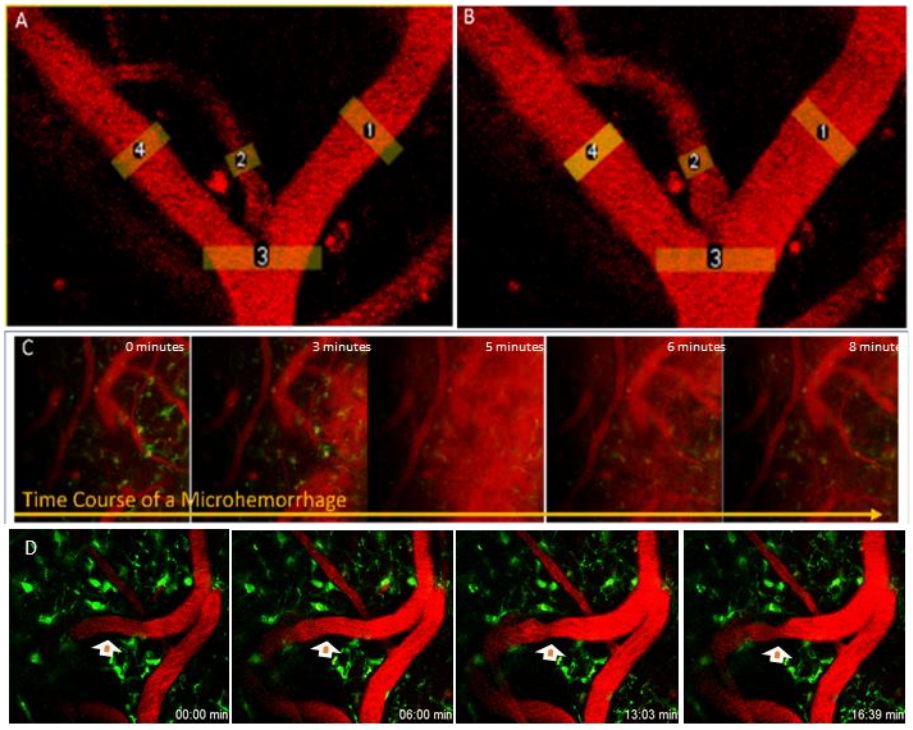

E

Acute NNK Vascular Events	PBS n=3	NNK n=5
Vasodilation	11%	42%
Vasoconstriction	0%	26%
Microhemorrhage	0%	47%
Any Vascular Events	**11%**	**72%**

Figure 17: Vessel dynamic changes in time series. A & B) Representative images of vessel dynamics in NNK treated mice. Vasodilation was noted and lines (1-4) were added for the distinction of vessel diameter change. C) NNK exposed mice also revealed microhemorrhaging, the last 2 panels show apparent clearing of leaked blood. D)Vasoconstriction was observed and sustained for more than 3 minutes. No hemorrhage was noted at this site. E) Tabulation of vascular events observed in all samples. A comparison of control to NNK shows distinct separation between the two groups. No events of vasoconstriction or microhemorrhage were observed in control subjects. Evans Blue labeled vessels are represented in re and microglia in green for all images.

Continuous Treatment with NNK Maintains Increased Vascular Events and Microhemorrhages

We next analyzed the effects of chronic treatment with NNK on vessel dynamics. Similarly, to acute treatment, vascular events of all types increased with NNK treatment, compared to the PBS group, while an increase in the co-occurrence of events was also observed (Fig. 18). For the PBS group, we noted that 11% of the sites had events of vasodilation, 11% of the sites had an event of vasoconstriction and 11% of the sites had an event of microhemorrhage (Fig. 18B). Events of vasoconstriction and vasodilation are common events that are present under normal conditions and microhemorrhages can point to an effect of aging.[126] In the NNK group 20% of the sites had an event of vasodilation, 60% of the sites had an event of vasoconstriction and 67% of the sites had an event of microhemorrhages (Fig 18B). Interestingly, in the chronic NNK treated group vasoconstriction and microhemorrhages became more common with spasm-like events becoming more apparent (Fig. 18A).

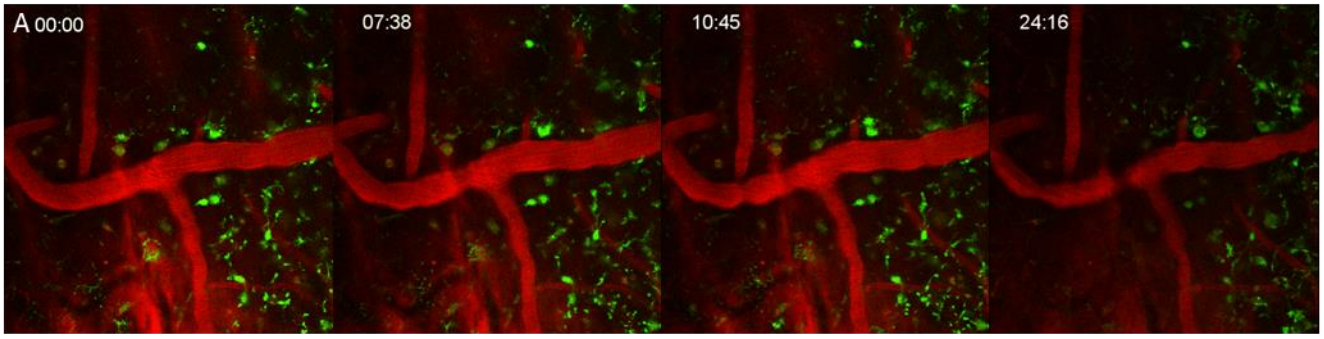

B

Chronic NNK Vascular Events	PBS n=3	NNK n=4
Vasodilation	11%	20%
Vasoconstriction	11%	60%
Microhemorrhage	11%	67%
Any Vascular Events	**33%**	**80%**

Figure 18: Vascular events seen in chronically NNK treated mice. A) Representative images of vessels going through multiple vascular events (vasodilation, vasoconstriction, and microhemorrhage). B) Tabulation of vascular events in PBS vs NNK. NNK group saw a sharp increase when compared to PBS. Evans Blue labeled vessels are represented in re and microglia in green for all images.

Immunofluorescence of Acutely NNK Treated Samples Shows Microglia Morphological Changes

In order to expand and corroborate findings from *in vivo* experiments, we performed immunofluorescence staining of thin tissue sections for various markers and retained the GFP signal in microglia (Fig. 19). Whole stitched sagittal sections were imaged and revealed a variety of microglia morphological states (ramified to ameboid) appeared to be widespread in the NNK group while the PBS group showed mostly surveying microglia (Fig. 19A & B). Imaging in the prefrontal cortical region revealed that microglia morphology was similar to that of IVM findings with an increased number of ameboid and hyper ramified cells in the NNK treated group (Fig. 19F) while the PBS group showed the majority of the observed microglia in a surveying state (Fig. 19E). Interestingly, the NNK group showed fragmented microglia around the orbital area of the cortex close to the olfactory bulb (Fig. 19B, white arrow). Closer inspection of these areas showed small puncta with GFP signal, but larger bodies (like those of somas) were absent (Fig. 19D, GFP channel). Moreover, depletion of synaptic marker PSD95 was observed in this area as well (Fig. 19D) while the PBS group showed typical distribution (Fig. 19C). Staining of astrocyte marker GFAP appears to be more diffused in whole sagittal section imaging of the NNK group (Fig. 19A & B) but closer inspection with higher magnification shows similar distribution between the two groups (Fig. 19C & D). Grouping of microglia was also observed in the NNK group with various morphological stages (Fig. 19F, white arrows).

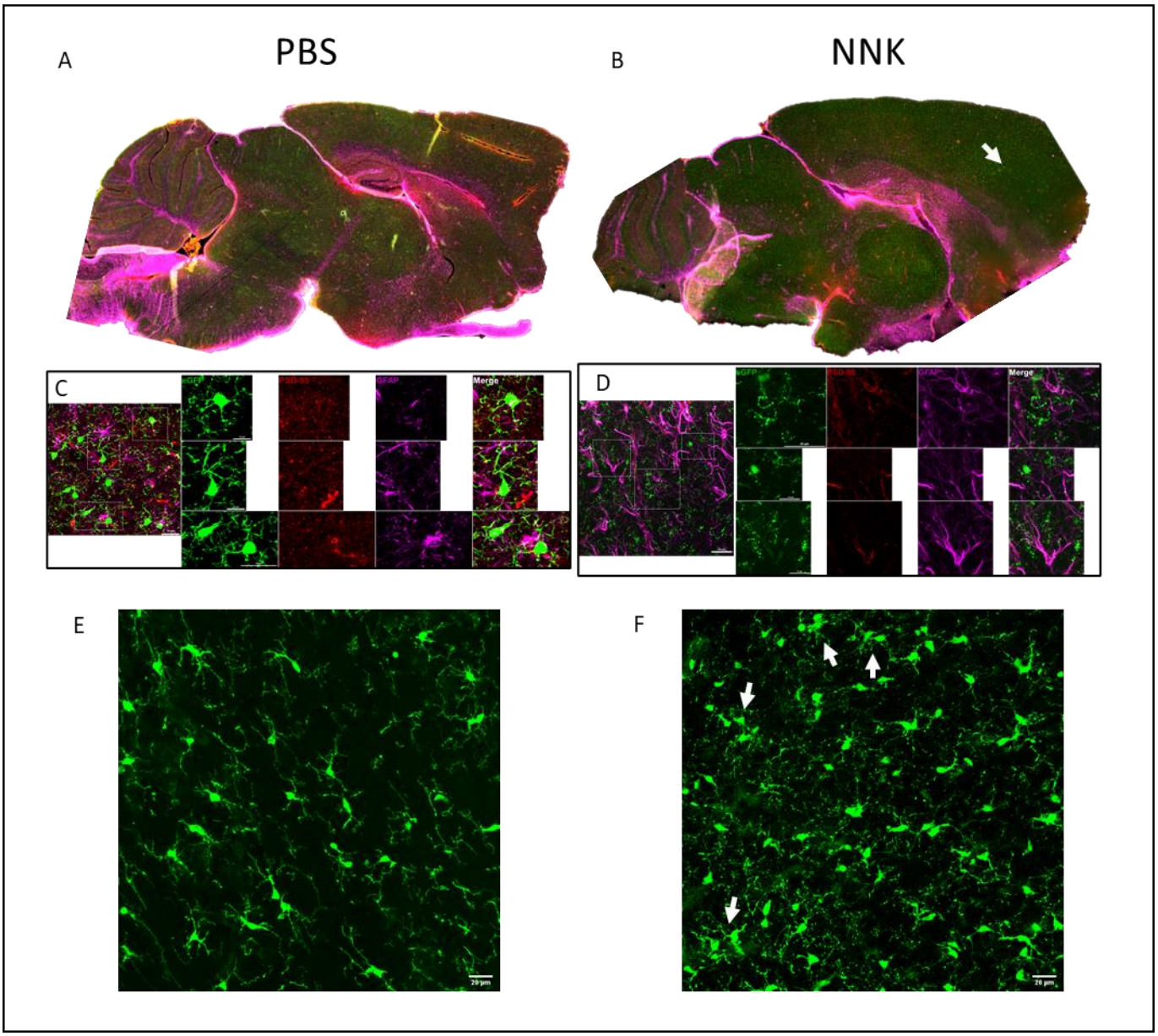

Figure 19: Representative immunofluorescence images of extracted tissue. A & B) whole sagittal section imaged at 5X with 3 channels (GFP-green, GFAP-magenta, PSD95-red). Stitched sagittal section showed heterogeneous microglia morphological states (ramified to ameboid) to be widespread in the NNK group while the PBS group displayed surveying microglia. White arrow points to a decreased signal of GFP expressing cells near the olfactory bulb. C & D) representative images of 40X imaging showing microglia, astrocyte, and synaptic distribution (scale bar-20µm). NNK-treated animals showed GFP positive puncta

while comparable regions in PBS treated showed typical microglia morphology. E & F) representative images of 20X imaging in cortical regions showing microglia morphology and distribution (scale bar-20 μm). White arrows show grouping of microglia somas in multiple regions.

Discussion

CS is the most significant source of toxicant exposure to humans with 1.3 billion current users worldwide of which up to half are expected to die from CS-related complications .[127] NNK is one of the most important oncogenic chemicals found in CS as it has been shown to have effects linked to multiple forms of cancers, cardiovascular disease, and neuronal damage.[33, 109, 128, 129] As NNK can also be found in e-cigarettes and has been shown to cause damages similar to that of CS, it becomes imperative to better understand the potential damages that it might be causing in organ systems that have received limited attention.[130] Current understanding of the mechanism of insult done by NNK in the brain involves the promotion of proinflammatory effector proteins in microglia and astrocytes with subsequent neuronal damage.[109] However, no effort has been made to understand the cascade of events that leads NNK molecules into the immunoprivileged space of the brain.

Previously, IP delivery with NNK for 4 and 12 days was shown to induce activation of microglia in cell culture and in histology from a mouse preclinical model. Effects seen in this study included upregulation of proinflammatory cytokines and an increase in ROS and nitric oxide (NO).[109] These offer a potential mode of action as to how progressive damage by NNK exposure can lead to disruption of the BBB and subsequent neuroinflammatory effects. As NNK is highly lipid-soluble, it is likely that it can cross the plasma membrane of cells it comes in contact with and potentially cross the BBB.[131] During an inflammatory event, the BBB may go through disruptive changes that lead to the opening of the barrier allowing the content of the vessels to flow into neural tissue.[132] Adding the increased ROS stress and signaling of NO for vessel dilation can further deteriorate the BBB leading to further opening. It is likely that the additive effects of this toxicant can be observed *in vivo* by inspecting for inflammatory events and BBB disruption.

In this study, we investigated the effects of NNK on both microglia and vessels in an acute and chronic intranasal delivery model. To better understand the potential effects of NNK, we developed an intranasal

delivery method on the *CX$_3$CR-1^{GFP}* mouse model to mimic inhalation exposure. NNK was delivered intranasally at 0.5 mg/kg in both acute (4 days) and chronic (12 weeks), we then performed thinned skull cranial window for intravital imaging. Using the GFP signal for microglia and Evans Blue for vessel, we were able to visualize spatiotemporal dynamics of NNK exposure. To further probe the effects, we used large tissue labeling and imaging and thin section staining.

The value of *in vivo* studies is the ability to see microglia and vessel dynamics, including their real-time interactions, when treating with acute and chronic intranasal NNK treatment, something not previously seen. Additionally, full-field 3D segmentation and quantification of different morphological features (microglial soma, processes, as well as their respective uptake capability and surrounding vasculature) give better insight into their functions and behavior when disrupted by NNK treatment. The spatial analysis also lends a new perspective of potential functional patterns microglia may have when located farther or near vasculature.

The microglial changes found with acute NNK treatment show similar signs of neuroinflammatory morphology that have been shown in other studies with brain pathology.[60, 133, 134] These include soma morphological changes that have only been previously analyzed in 2D.[65] Indeed, we observed similar morphological changes in 2D data with an increase in activated microglia and a positive association in the acutely treated NNK group (Fig. 14A & B). An increase in the frequency of larger somas in acutely NNK treated animals was also observed, while control showed a higher percentage in smaller volumes (Fig. 13E). Plotting of microglia soma in a box plot showed the heterogeneity of soma volumes within the data set and, importantly, displayed an increase in soma volume overall in acutely NNK treated animals (Fig. 13F). Moreover, increased somas sizes were qualitatively associated with hypertrophied processes and ameboid over ramified microglia. Quantitative analysis of this morphological comparison is ongoing. Plotting of the soma distance to vessel revealed a shorter average distance in the acutely treated NNK group (Fig. 13G). To understand this effect of NNK, we further analyzed soma distances to vessels by grouping them into three categories, Contact, Close and Far and performed an association analysis using chi square test of

independence (Fig. 15E). We noted that the acutely treated group had a positive association with Contact and Close classification and a negative association with Far while PBS showed the opposite behavior (Fig. 15E). A closer association of microglia somas to vessels might indicate a potential pathological event that requires the involvement of microglia which could include pro-inflammatory signaling and/or phagocytosis.

Interestingly, when we performed these analyses on our chronic data we observed similar trends (Fig. 16). However, slight differences were observed in association in the Close classification for the three-classification analysis, with chronically NNK treated showing a negative association while chronically treated PBS showed a positive association (Fig. 16A). This can potentially point to microglia that were previously in the Close group in acute shifting to either the Far or Contact group suggesting migratory behavior of microglia toward injury sites that has been seen in other studies.[135, 136] Quantitative analysis of this behavior is ongoing. In the distance to vessel box plot of chronic data, we can also observe a clustering of somas at closer distances in the PBS data (Fig. 16E).

VAM and increased soma size have been observed in cerebrovascular dysfunction and neurodegenerative disorders.[65, 125, 137] Our study indicates that treatment with acute and chronic NNK can lead to increased grouping of microglia somas with vessels along with increased average soma volume (Fig. 13-16). This is indicative of microglia activity near vasculature due to a potential insult caused by exposure to NNK. The microglia's ability to engulf and process neuronal infiltrates shows a strong indication that these cells are in fact responding to toxicant exposure effects and possibly to the toxicant itself.[138] Moreover, the capacity of microglia to signal for proinflammatory events can lead to potential exacerbation of collection of cells along the vessels created by the milieu of proinflammatory cytokines produced at the site.[139] Previous studies have shown that up to 33% of microglia can associate with vessels under normal conditions, as visualized by full cranial window imaging, and that signaling from vasculature can modulate the amount of microglia interaction which is reflective of our data.[137] However, the increased association of these microglia somas with activated morphology in NNK treatment groups indicates that cellular

signaling from either microglia or other neighboring cells can modulate the amount of VAMs and potentially reach a stable homeostatic level of association with vessels (Fig. 15E & 16A). To corroborate the *in vivo* findings, we also performed *ex vivo* staining on thin and thick tissue with multiple relevant markers. The approach taken in this study offers an innovative procedure to probe the effects of NNK on microglia and the BBB to reveal novel information about the insult.

Another finding of interest is the apparent dilation of vasculature in NNK treated mice an observation that has been found in a variety of disorders showing vascular dysfunction[140].

Previous studies have shown the role of CS in brain vascular pathology by the involvement of nAChRs and OxS.[141, 142] This is in part due to molecules, such as NNK, that can bind and activate nAChRs and OxS generated from this and other pathways.[33, 44] Exposure of the brain to NNK can, therefore, be expected to induce vascular effects that can have detrimental outcomes given that NNK can both bind to nAChRs and generate OxS. Indeed, our study shows that NNK treatment, whether acute or chronic, can induce a diverse set of vascular events (Fig. 15 & 18). In acutely treated animals we see an increase in all vascular events including vasodilation, vasoconstriction, and microhemorrhages while chronic treatment saw a similar increase when compared to PBS (Fig. 17E & Fig. 18B). Although vasoconstriction and vasodilation are not always detrimental, a collective increase of these events followed by microhemorrhages can point to underlying pathological causes, in this case, the introduction of NNK. Interestingly, when acute and chronic NNK groups were compared, an increase in vasoconstriction and microhemorrhages were observed in the chronic group but not in vasodilation (Fig. 17E & Fig. 18B).

As NNK molecules can travel through the circulatory system and freely cross the plasma membrane, it is likely that exposure of the BBB to NNK can lead to the events observed in this study.[131] A potential sequence of events leading to these effects can include the freely circulating NNK coming into contact with endothelial cells of the BBB and activating nAChRs inducing metabolic activity while a portion of the NNK molecules can also cross the plasma membrane and create DNA adducts. These can then cause aberrant cell function that may lead to the disruption of components such as TJs. In such a case,

the BBB can be compromised leading to potential transient opening and spillage of the vessel content into neural tissue. The ability of certain nAChRs to signal for vasoconstriction and vasodilation may further exacerbate the microhemorrhages events.[142, 143] Our data shows that events consistent with the above, suggest events are in fact happening in NNK treated subjects (Fig. 17 & 18). Ongoing studies aim to evaluate the role of TJs, OxS, and DNA adducts damage.

Due to different metabolic requirements and neurotransmitter activity of the brain, blood flow might be increased in some regions compared to others and shift over time.[144] This could mean that circulating toxins, such as NNK, can be deposited in some areas at one point and shift to other areas at another point potentially causing widespread damage over time. Our thin tissue imaging shows that microglia ameboid morphology is outspread (Fig. 19). Moreover, other events of tissue damage can be seen through immunofluorescence staining such as depletion of PSD95 showing potential synaptic damage and fragmentation of microglia (Fig. 19C & D). Microglia-associated synaptic loss has been linked to neurodegenerative disorders and traumatic brain injury in previous studies pointing to a potential link between NNK insult and our observed effects.[145, 146] Loss of PSD95 has been linked to neuronal damage or disfunction making it a good target for assessment of neuronal insult.[147, 148]

Collectively, the observed effects of NNK treatment on microglia and vessels, suggest that the damage caused is a stepwise process but could be influenced by NNK crossing the plasma membrane, eventually finding its way into neural tissue. However, a buildup of enough NNK concentration in the circulating blood would have to occur first for this route to have a significant contribution. Traffic of NNK particles through the circulatory system reaches the BBB and interacts with endothelial cells causing disfunction of the barrier. The content of the vessels can flood into neural tissue and interact with surrounding cells. As the resident immune cells of the brain, microglia respond to the influx of infiltrates and begin to morph into their activated form while potentially releasing signaling molecules such as proinflammatory cytokines. While cytokines were not measured in this study, a prior microglial culture study showed that NNK exposure leads to microglia release of cytokines. These can potentially have

detrimental effects on normal functions such as synaptic pruning and cell viability. While these events might be mild and reparable with limited exposure, repeated exposures over long periods of time can potentially cause significant damage and might be a factor in the progression of preexisting pathologies such as neurodegenerative diseases. A graphical representation of our proposed model can be seen in Figure 20.

In this study, we were able to show that acute treatment with NNK via intranasal delivery yields quantifiable effects visible with *in vivo* thinned skull cranial window. These effects include microglial responses and BBB disruption. NNK being a molecule that is present in nicotine products either by combustion[32] or by synthesis within the cell after uptake of nicotine[33] is a molecule of interest to study the potentially detrimental effects of cigarette smoking or e-cigarette usage. Development of methods for the detection and tracking of damage caused by such molecules are necessary. While our study demonstrates the potential of IVM as a tool for the toxicological assessment of CS molecules, such as NNK, further studies are needed to understand molecular key players in the path of damage caused. Intranasal delivery offers a method of delivery that more closely resembles the typical exposure of NNK when compared to other widely used methods such as IP delivery.[149] This method exposed the subjects directly through the respiratory system and delivers NNK straight to the lungs, unlike IP which relies on the eventual circulation of the toxicant to reach targeted organs. Additionally, intranasal delivery can incorporate aspects of 2nd and 3rd hand smoke exposure that are inevitable for users of nicotine products (Wei et al. 2015). However, limitations exist, as intranasal delivery in an animal model that is obligate nasal breathers do not completely encapsulate mouth exposure in humans.

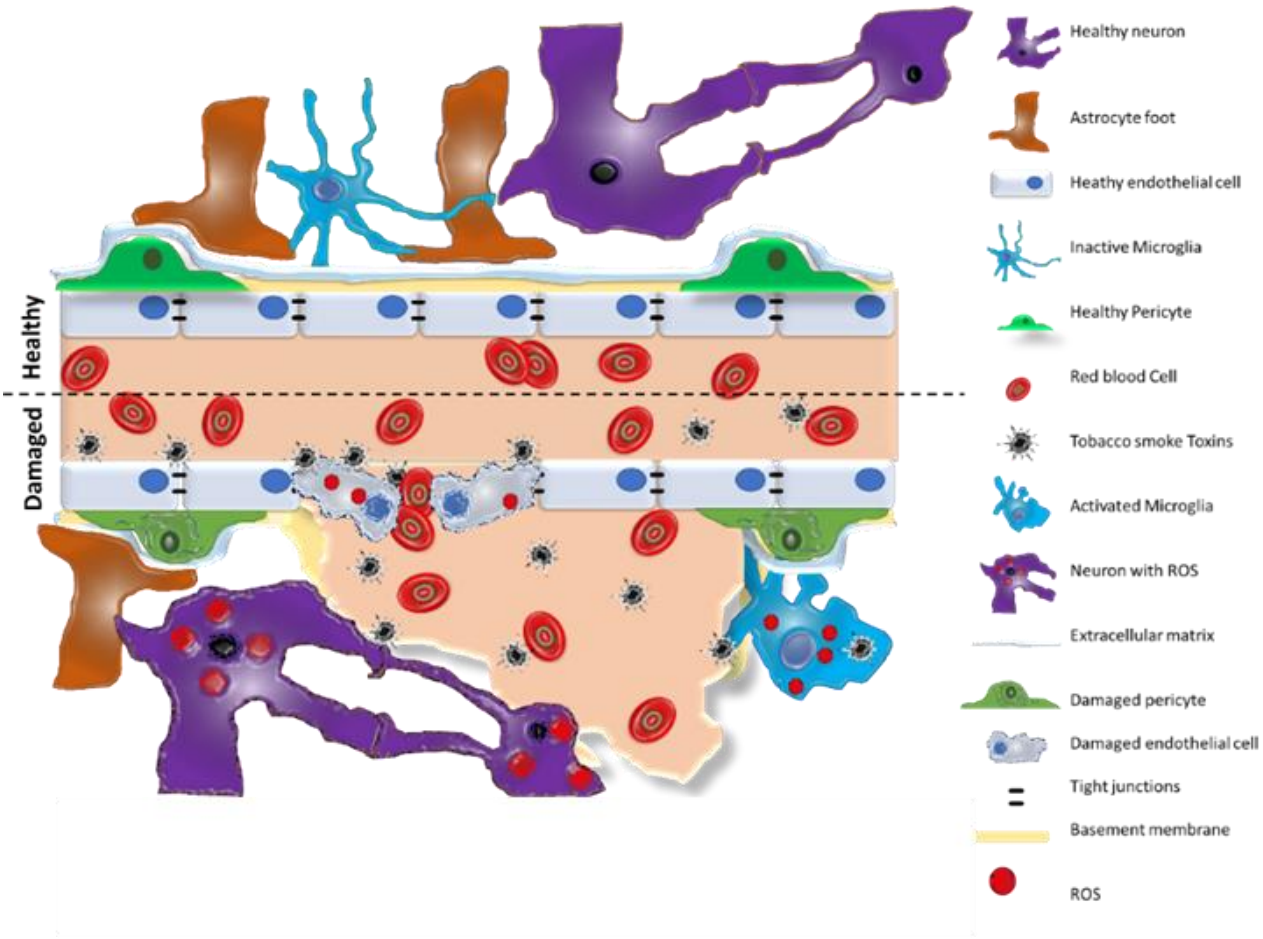

Figure 20: Schematic representation of the proposed model. Under normal conditions, the BBB controls the traffic of molecules from circulating blood into neural tissue (top). The introduction of toxicants interacts with endothelial cells inducing cellular damage and creating ROS stress. Sustained OxS leads to TJ dysfunction and opening of BBB. The content of vessels can then spill into neural tissue and the content of vessels interact with neuronal cells including microglia inducing activation and morphological changes (bottom).

Chapter V: Conclusions and future direction

The prevalence of Tobacco product use is an imminent issue affecting the entire world and it's the leading cause of death, illness, and impoverishment worldwide.[127] These types of products not only affect the user but can also affect those close to the source and unsuspecting victims that may come in contact with surfaces exposed to fumes produced.[2, 150] It is often the case that studies focus on stark pathologies of exposure and ignore more subtle effects. For example, studies exploring the oncogenicity of chemicals, like NNK, have tumor formation and genetic mutations as endpoints. However, there are some studies that have focused on understanding the effects from prolonged low exposures in various organs, like the lung.[35, 151-153] NNK is one of the major contenders for deleterious effects in nicotine products. NNK owes its hazard to its' chemistry and biological interactions which allows it to modulate cell behavior and freely move in and out of the cell.[33]

In this study, we investigated the effects of NNK delivered through the intranasal route at an acute and chronic regiment. We observed its effects *in vivo* through IVM and confirmed findings through immunofluorescence imaging. Our results show that NNK treatment, whether it is acute or chronic, yields microglial and vessel effects. These are more pronounced in the chronic treatment indicating an additive effect over time. Previous studies have shown that pro-inflammatory cytokines are released in microglia with activated morphology.[60, 69, 70, 139] The morphological changes observed in microglia indicate that a response to treatment can lead to potential pro-inflammatory signaling. However, the added observed effect detected in the vessels suggests that these changes are likely for preservation and not simply for maintenance. Under normal conditions, microglia can regulate vascular structure and function without morphological changes (Bisht et al 2021) but a shift in morphology coupled with grouping along the vessel has been shown to be associated with disease and injury.[125]

Future endeavors include further processing of different aspects of the microglia such as that of the involvement of the processes. Moreover, dynamic data from microglia time-series recordings are under

analysis. These include soma and projections data along with uptake of infiltrates. Time resolve information has the potential to further reveal the intimate relationship between microglia, vessels, and insult.

Other future studies can include the use of molecular markers to investigate the different states of microglia as it relates to morphology, such as proinflammatory states when treated with NNK. These studies can also link to potential damages caused in other cell types and their components. The involvement of endothelial cells and TJs play an important role in BBB function and understanding the state of these during NNK treatment can reveal further relevant information. Given that NNK has been linked to DNA adduct formation and nAChRs activation, additional studies could be conducted to understand if the distribution of DNA damage is linked to the distribution of nAChRs throughout the brain. The investigations of these could also help elucidate a potential mechanistic link to neurodegenerative disorders and tobacco usage as it has been noted in epidemiological studies.

Together, our data shows that NNK treatment has a marked effect on microglia and the BBB. The nature of the insult indicates that these effects can potentially interfere with normal function and lead to aggravated effects of underlying pathologies.

References

1. Ng M, Freeman MK, Fleming TD, Robinson M, Dwyer-Lindgren L, Thomson B, Wollum A, Sanman E, Wulf S, Lopez AD, Murray CJ, Gakidou E. Smoking prevalence and cigarette consumption in 187 countries, 1980-2012. Jama. 2014;311(2):183-92. Epub 2014/01/09. doi: 10.1001/jama.2013.284692. PubMed PMID: 24399557.
2. Centers for Disease Control Prevention HP, Office on Smoking Health. Health Effects of Secondhand Smoke 2020 [cited 2022]. Available from: https://www.cdc.gov/tobacco/data_statistics/fact_sheets/secondhand_smoke/health_effects/index.htm.
3. Boksa P. Smoking, psychiatric illness and the brain. Journal of psychiatry & neuroscience : JPN. 2017;42(3):147-9. doi: 10.1503/jpn.170060. PubMed PMID: 28440208.
4. Prochaska JJ, Das S, Young-Wolff KC. Smoking, Mental Illness, and Public Health. Annual review of public health. 2017;38:165-85. Epub 2016/12/16. doi: 10.1146/annurev-publhealth-031816-044618. PubMed PMID: 27992725.
5. Alrouji M, Manouchehrinia A, Gran B, Constantinescu CS. Effects of cigarette smoke on immunity, neuroinflammation and multiple sclerosis. LID - S0165-5728(18)30130-9 [pii] LID - 10.1016/j.jneuroim.2018.10.004 [doi](1872-8421 (Electronic)).
6. Mazzone P, Tierney W, Hossain M, Puvenna V, Janigro D, Cucullo L. Pathophysiological impact of cigarette smoke exposure on the cerebrovascular system with a focus on the blood-brain barrier: expanding the awareness of smoking toxicity in an underappreciated area. International journal of environmental research and public health. 2010;7(12):4111-26. Epub 2010/11/26. doi: 10.3390/ijerph7124111. PubMed PMID: 21317997.
7. Galasko D, Montine TJ. Biomarkers of oxidative damage and inflammation in Alzheimer's disease. Biomarkers in medicine. 2010;4(1):27-36. doi: 10.2217/bmm.09.89. PubMed PMID: 20383271.
8. Levin ED. Complex relationships of nicotinic receptor actions and cognitive functions. Biochemical pharmacology. 2013;86(8):1145-52. Epub 2013/08/06. doi: 10.1016/j.bcp.2013.07.021. PubMed PMID: 23928190.
9. Seo SB, Choe ES, Kim KS, Shim SM. The effect of tobacco smoke exposure on the generation of reactive oxygen species and cellular membrane damage using co-culture model of blood brain barrier with astrocytes. Toxicology and industrial health. 2017;33(6):530-6. Epub 2017/01/28. doi: 10.1177/0748233716687708. PubMed PMID: 28125953.
10. Swan GE, Lessov-Schlaggar CN. The Effects of Tobacco Smoke and Nicotine on Cognition and the Brain. Neuropsychology Review. 2007;17(3):259-73. doi: 10.1007/s11065-007-9035-9.
11. Saha SP, Bhalla DK, Whayne TF, Jr., Gairola C. Cigarette smoke and adverse health effects: An overview of research trends and future needs. Int J Angiol. 2007;16(3):77-83. doi: 10.1055/s-0031-1278254. PubMed PMID: 22477297.
12. Centers for Disease Control Prevention HP, Office on Smoking Health. Publications and Reports of the Surgeon General. How Tobacco Smoke Causes Disease: The Biology and Behavioral Basis for Smoking-Attributable Disease: A Report of the Surgeon General. Atlanta (GA): Centers for Disease Control and Prevention (US); 2010.
13. Shimada T, Fujii-Kuriyama Y. Metabolic activation of polycyclic aromatic hydrocarbons to carcinogens by cytochromes P450 1A1 and 1B1. Cancer Sci. 2004;95(1):1-6. Epub 2004/01/15. doi: 10.1111/j.1349-7006.2004.tb03162.x. PubMed PMID: 14720319.
14. Rodriguez-Antona C, Ingelman-Sundberg M. Cytochrome P450 pharmacogenetics and cancer. Oncogene. 2006;25(11):1679-91. doi: 10.1038/sj.onc.1209377.

15. Xue J, Yang S, Seng S. Mechanisms of Cancer Induction by Tobacco-Specific NNK and NNN. Cancers (Basel). 2014;6(2):1138-56. doi: 10.3390/cancers6021138. PubMed PMID: 24830349.
16. Wiencke JK. DNA adduct burden and tobacco carcinogenesis. Oncogene. 2002;21(48):7376-91. Epub 2002/10/16. doi: 10.1038/sj.onc.1205799. PubMed PMID: 12379880.
17. Lucas A, Yasa J, Lucas M. Regeneration and repair in the healing lung. Clin Transl Immunology. 2020;9(7):e1152-e. doi: 10.1002/cti2.1152. PubMed PMID: 32665845.
18. Arcavi L, Benowitz NL. Cigarette Smoking and Infection. Archives of Internal Medicine. 2004;164(20):2206-16. doi: 10.1001/archinte.164.20.2206.
19. Rahman I, Biswas SK, Kode A. Oxidant and antioxidant balance in the airways and airway diseases. Eur J Pharmacol. 2006;533(1-3):222-39. Epub 2006/02/28. doi: 10.1016/j.ejphar.2005.12.087. PubMed PMID: 16500642.
20. Bowler RP, Barnes PJ, Crapo JD. The role of oxidative stress in chronic obstructive pulmonary disease. Copd. 2004;1(2):255-77. Epub 2006/12/02. doi: 10.1081/copd-200027031. PubMed PMID: 17136992.
21. Demizu Y, Sasaki R, Trachootham D, Pelicano H, Colacino JA, Liu J, Huang P. Alterations of cellular redox state during NNK-induced malignant transformation and resistance to radiation. Antioxid Redox Signal. 2008;10(5):951-61. doi: 10.1089/ars.2007.1871. PubMed PMID: 18257743.
22. Nishioka T, Guo J, Yamamoto D, Chen L, Huppi P, Chen CY. Nicotine, through upregulating pro-survival signaling, cooperates with NNK to promote transformation. J Cell Biochem. 2010;109(1):152-61. doi: 10.1002/jcb.22392. PubMed PMID: 19911375.
23. Food and Drug Administration. How Smoking Affects Heart Health 2022. Available from: https://www.fda.gov/tobacco-products/health-effects-tobacco-use/how-smoking-affects-heart-health.
24. Messner BB, David. Mechanisms of Endothelial Dysfunction and Early Atherogenesis Arteriosclerosis, Thrombosis, and Vascular Biology2014 [cited 2022]. Available from: https://www.ahajournals.org/doi/10.1161/atvbaha.113.300156.
25. Barua RS, Ambrose JA, Eales-Reynolds LJ, DeVoe MC, Zervas JG, Saha DC. Dysfunctional endothelial nitric oxide biosynthesis in healthy smokers with impaired endothelium-dependent vasodilatation. Circulation. 2001;104(16):1905-10. Epub 2001/10/17. doi: 10.1161/hc4101.097525. PubMed PMID: 11602492.
26. Hayyan M, Hashim MA, AlNashef IM. Superoxide Ion: Generation and Chemical Implications. Chemical Reviews. 2016;116(5):3029-85. doi: 10.1021/acs.chemrev.5b00407.
27. Beckman JS, Koppenol WH. Nitric oxide, superoxide, and peroxynitrite: the good, the bad, and ugly. Am J Physiol. 1996;271(5 Pt 1):C1424-37. Epub 1996/11/01. doi: 10.1152/ajpcell.1996.271.5.C1424. PubMed PMID: 8944624.
28. Sheweita SA, El-Bendery HA, Mostafa MH. Novel Study on N-Nitrosamines as Risk Factors of Cardiovascular Diseases. BioMed Research International. 2014;2014:817019. doi: 10.1155/2014/817019.
29. Chatterjee S, Tao JQ, Johncola A, Guo W, Caporale A, Langham MC, Wehrli FW. Acute exposure to e-cigarettes causes inflammation and pulmonary endothelial oxidative stress in nonsmoking, healthy young subjects. Am J Physiol Lung Cell Mol Physiol. 2019;317(2):L155-l66. Epub 2019/05/02. doi: 10.1152/ajplung.00110.2019. PubMed PMID: 31042077; PMCID: PMC6734380.
30. Kelesidis T, Tran E, Nguyen R, Zhang Y, Sosa G, Middlekauff HR. Association of 1 Vaping Session With Cellular Oxidative Stress in Otherwise Healthy Young People With No History of Smoking or Vaping: A Randomized Clinical Crossover Trial. JAMA Pediatrics. 2021;175(11):1174-6. doi: 10.1001/jamapediatrics.2021.2351.
31. Kuntic M, Oelze M, Steven S, Kröller-Schön S, Stamm P, Kalinovic S, Frenis K, Vujacic-Mirski K, Bayo Jimenez MT, Kvandova M, Filippou K, Al Zuabi A, Brückl V, Hahad O, Daub S, Varveri F, Gori T, Huesmann R, Hoffmann T, Schmidt FP, Keaney JF, Jr., Daiber A, Münzel T. Short-term e-cigarette vapour exposure causes vascular oxidative stress and dysfunction: evidence for a close connection to brain

damage and a key role of the phagocytic NADPH oxidase (NOX-2). European Heart Journal. 2020;41(26):2472-83. doi: 10.1093/eurheartj/ehz772.
32. Sleiman M, Gundel LA, Pankow JF, Jacob P, 3rd, Singer BC, Destaillats H. Formation of carcinogens indoors by surface-mediated reactions of nicotine with nitrous acid, leading to potential thirdhand smoke hazards. Proc Natl Acad Sci U S A. 2010;107(15):6576-81. Epub 2010/02/08. doi: 10.1073/pnas.0912820107. PubMed PMID: 20142504.
33. Hecht SS. Biochemistry, Biology, and Carcinogenicity of Tobacco-Specific N-Nitrosamines. Chemical Research in Toxicology. 1998;11(6):559-603. doi: 10.1021/tx980005y.
34. Hu SC, Bryant MS, Sepehr E, Kang HK, Trbojevich R, Lagaud G, Mehta D, Ding W, Mittelstaedt RA, Pearce MG, Bishop ME, Davis KJ, Lewis SM, Chemerynski S, Yee SB, Coraggio M, Rosenfeldt H, Yeager RP, Howard PC, Tang Y. Toxicokinetic and Genotoxicity Study of NNK in Male Sprague Dawley Rats Following Nose-Only Inhalation Exposure, Intraperitoneal Injection, and Oral Gavage. Toxicol Sci. 2021;182(1):10-28. Epub 2021/05/05. doi: 10.1093/toxsci/kfab049. PubMed PMID: 33944952.
35. Hu SC, Min S, Kang HK, Yang DJ, Lewis SM, Davis KJ, Patton RE, Bryant MS, Sepehr E, Trbojevich R, Pearce MG, Bishop ME, Heflich RH, Maisha MP, Felton R, Chemerynski S, Yee SB, Coraggio M, Rosenfeldt H, Yeager RP, Howard PC, Tang Y. 14-Day Nose-Only Inhalation Toxicity and Haber's Rule Study of NNK in Sprague-Dawley Rats. Toxicol Sci. 2021;183(2):319-37. Epub 2021/07/31. doi: 10.1093/toxsci/kfab094. PubMed PMID: 34329464.
36. Jansen JG, de Groot AJ, van Teijlingen CM, Tates AD, Vrieling H, van Zeeland AA. Induction of hprt gene mutations in splenic T-lymphocytes from the rat exposed in vivo to DNA methylating agents is correlated with formation of O6-methylguanine in bone marrow and not in the spleen. Carcinogenesis. 1996;17(10):2183-91. Epub 1996/10/01. doi: 10.1093/carcin/17.10.2183. PubMed PMID: 8895487.
37. Povey AC, Badawi AF, Cooper DP, Hall CN, Harrison KL, Jackson PE, Lees NP, O'Connor PJ, Margison GP. DNA alkylation and repair in the large bowel: animal and human studies. J Nutr. 2002;132(11 Suppl):3518s-21s. Epub 2002/11/08. doi: 10.1093/jn/132.11.3518S. PubMed PMID: 12421880.
38. Somm E. Nicotinic Cholinergic Signaling in Adipose Tissue and Pancreatic Islets Biology: Revisited Function and Therapeutic Perspectives. Archivum Immunologiae et Therapiae Experimentalis. 2014;62(2):87-101. doi: 10.1007/s00005-013-0266-6.
39. Zhao Y. The Oncogenic Functions of Nicotinic Acetylcholine Receptors. J Oncol. 2016;2016:9650481-. Epub 2016/02/14. doi: 10.1155/2016/9650481. PubMed PMID: 26981122.
40. Schuller HM. Is cancer triggered by altered signalling of nicotinic acetylcholine receptors? Nat Rev Cancer. 2009;9(3):195-205. Epub 2009/02/06. doi: 10.1038/nrc2590. PubMed PMID: 19194381.
41. Wang S, Hu Y. α7 nicotinic acetylcholine receptors in lung cancer. Oncol Lett. 2018;16(2):1375-82. Epub 2018/05/30. doi: 10.3892/ol.2018.8841. PubMed PMID: 30008813.
42. Feduccia A, Chatterjee S, Bartlett S. Neuronal nicotinic acetylcholine receptors: neuroplastic changes underlying alcohol and nicotine addictions. Frontiers in Molecular Neuroscience. 2012;5. doi: 10.3389/fnmol.2012.00083.
43. Schuller HM, Al-Wadei HA, Majidi M. Gamma-aminobutyric acid, a potential tumor suppressor for small airway-derived lung adenocarcinoma. Carcinogenesis. 2008;29(10):1979-85. Epub 2008/03/04. doi: 10.1093/carcin/bgn041. PubMed PMID: 18310090; PMCID: PMC2556972.
44. Singh S, Pillai S, Chellappan S. Nicotinic acetylcholine receptor signaling in tumor growth and metastasis. J Oncol. 2011;2011:456743. Epub 2011/05/05. doi: 10.1155/2011/456743. PubMed PMID: 21541211; PMCID: PMC3085312.
45. Rosa JG, Prokopczyk B, Desai DH, Amin SG, El-Bayoumy K. Elevated 8-hydroxy-2'-deoxyguanosine levels in lung DNA of A/J mice and F344 rats treated with 4-(methylnitrosamino)-1-(3-pyridyl)-1-butanone and inhibition by dietary 1,4-phenylenebis(methylene)selenocyanate.

Carcinogenesis. 1998;19(10):1783-8. Epub 1998/11/07. doi: 10.1093/carcin/19.10.1783. PubMed PMID: 9806159.
46. Hecht SS. DNA adduct formation from tobacco-specific N-nitrosamines. Mutat Res. 1999;424(1-2):127-42. Epub 1999/03/05. doi: 10.1016/s0027-5107(99)00014-7. PubMed PMID: 10064856.
47. Kankanamage RNT, Ghosh AB, Jiang D, Gkika K, Keyes T, Achola LA, Suib S, Rusling JF. Metabolites of Tobacco- and E-Cigarette-Related Nitrosamines Can Drive Cu(2+)-Mediated DNA Oxidation. Chem Res Toxicol. 2020;33(8):2072-86. Epub 2020/07/17. doi: 10.1021/acs.chemrestox.0c00027. PubMed PMID: 32672941; PMCID: PMC7510339.
48. Therriault MJ, Proulx LI, Castonguay A, Bissonnette EY. Immunomodulatory effects of the tobacco-specific carcinogen, NNK, on alveolar macrophages. Clin Exp Immunol. 2003;132(2):232-8. doi: 10.1046/j.1365-2249.2003.02142.x. PubMed PMID: 12699410.
49. Dome P, Lazary J, Kalapos MP, Rihmer Z. Smoking, nicotine and neuropsychiatric disorders. Neurosci Biobehav Rev. 2010;34(3):295-342. Epub 2009/08/12. doi: 10.1016/j.neubiorev.2009.07.013. PubMed PMID: 19665479.
50. Anthony JC, Chen CY, Storr CL. Drug dependence epidemiology. Clinical Neuroscience Research. 2005;5(2):55-68. doi: https://doi.org/10.1016/j.cnr.2005.08.002.
51. Piasecki TM. Relapse to smoking. Clinical Psychology Review. 2006;26(2):196-215. doi: https://doi.org/10.1016/j.cpr.2005.11.007.
52. Campos MW, Serebrisky D, Castaldelli-Maia JM. Smoking and Cognition. Curr Drug Abuse Rev. 2016;9(2):76-9. Epub 2016/08/06. doi: 10.2174/1874473709666160803101633. PubMed PMID: 27492358.
53. Durazzo TC, Mattsson N, Weiner MW, Alzheimer's Disease Neuroimaging I. Smoking and increased Alzheimer's disease risk: a review of potential mechanisms. Alzheimers Dement. 2014;10(3 Suppl):S122-S45. doi: 10.1016/j.jalz.2014.04.009. PubMed PMID: 24924665.
54. Milatovic D, Zaja-Milatovic S, Breyer RM, Aschner M, Montine TJ. Chapter 55 - Neuroinflammation and Oxidative Injury in Developmental Neurotoxicity. In: Gupta RC, editor. Reproductive and Developmental Toxicology (Second Edition): Academic Press; 2017. p. 1051-61.
55. Li J-W, Zong Y, Cao X-P, Tan L, Tan L. Microglial priming in Alzheimer's disease. Annals of translational medicine. 2018;6(10):176-. doi: 10.21037/atm.2018.04.22. PubMed PMID: 29951498.
56. Perry VH, Nicoll JA, Holmes C. Microglia in neurodegenerative disease. Nature reviews Neurology. 2010;6(4):193-201. Epub 2010/03/18. doi: 10.1038/nrneurol.2010.17. PubMed PMID: 20234358.
57. Muzio L, Viotti A, Martino G. Microglia in Neuroinflammation and Neurodegeneration: From Understanding to Therapy. Front Neurosci. 2021;15:742065-. doi: 10.3389/fnins.2021.742065. PubMed PMID: 34630027.
58. Lawson LJ, Perry VH, Dri P, Gordon S. Heterogeneity in the distribution and morphology of microglia in the normal adult mouse brain. Neuroscience. 1990;39(1):151-70. doi: https://doi.org/10.1016/0306-4522(90)90229-W.
59. Nicholson LB. The immune system. Essays Biochem. 2016;60(3):275-301. doi: 10.1042/EBC20160017. PubMed PMID: 27784777.
60. Heindl S, Gesierich B, Benakis C, Llovera G, Duering M, Liesz A. Automated Morphological Analysis of Microglia After Stroke. Frontiers in Cellular Neuroscience. 2018;12. doi: 10.3389/fncel.2018.00106.
61. Sierra A, Encinas JM, Deudero JJP, Chancey JH, Enikolopov G, Overstreet-Wadiche LS, Tsirka SE, Maletic-Savatic M. Microglia Shape Adult Hippocampal Neurogenesis through Apoptosis-Coupled Phagocytosis. Cell Stem Cell. 2010;7(4):483-95. doi: https://doi.org/10.1016/j.stem.2010.08.014.
62. Kettenmann H, Kirchhoff F, Verkhratsky A. Microglia: New Roles for the Synaptic Stripper. Neuron. 2013;77(1):10-8. doi: https://doi.org/10.1016/j.neuron.2012.12.023.

63. Davalos D, Grutzendler J, Yang G, Kim JV, Zuo Y, Jung S, Littman DR, Dustin ML, Gan W-B. ATP mediates rapid microglial response to local brain injury in vivo. Nature Neuroscience. 2005;8(6):752-8. doi: 10.1038/nn1472.
64. Nimmerjahn A, Kirchhoff F, Helmchen F. Resting microglial cells are highly dynamic surveillants of brain parenchyma in vivo. Science. 2005;308(5726):1314-8. Epub 2005/04/16. doi: 10.1126/science.1110647. PubMed PMID: 15831717.
65. Davis BM, Salinas-Navarro M, Cordeiro MF, Moons L, De Groef L. Characterizing microglia activation: a spatial statistics approach to maximize information extraction. Scientific Reports. 2017;7(1):1576. doi: 10.1038/s41598-017-01747-8.
66. Fernández-Arjona MdM, Grondona JM, Granados-Durán P, Fernández-Llebrez P, López-Ávalos MD. Microglia Morphological Categorization in a Rat Model of Neuroinflammation by Hierarchical Cluster and Principal Components Analysis. Frontiers in Cellular Neuroscience. 2017;11. doi: 10.3389/fncel.2017.00235.
67. Kongsui R, Beynon SB, Johnson SJ, Walker FR. Quantitative assessment of microglial morphology and density reveals remarkable consistency in the distribution and morphology of cells within the healthy prefrontal cortex of the rat. Journal of Neuroinflammation. 2014;11(1):182. doi: 10.1186/s12974-014-0182-7.
68. Prinz M, Jung S, Priller J. Microglia Biology: One Century of Evolving Concepts. Cell. 2019;179(2):292-311. Epub 2019/10/05. doi: 10.1016/j.cell.2019.08.053. PubMed PMID: 31585077.
69. Silvin A, Ginhoux F. Microglia heterogeneity along a spatio-temporal axis: More questions than answers. Glia. 2018;66(10):2045-57. Epub 2018/08/26. doi: 10.1002/glia.23458. PubMed PMID: 30144321.
70. Li Q, Barres BA. Microglia and macrophages in brain homeostasis and disease. Nature Reviews Immunology. 2018;18(4):225-42. doi: 10.1038/nri.2017.125.
71. Ajami B, Samusik N, Wieghofer P, Ho PP, Crotti A, Bjornson Z, Prinz M, Fantl WJ, Nolan GP, Steinman L. Single-cell mass cytometry reveals distinct populations of brain myeloid cells in mouse neuroinflammation and neurodegeneration models. Nat Neurosci. 2018;21(4):541-51. Epub 2018/03/07. doi: 10.1038/s41593-018-0100-x. PubMed PMID: 29507414; PMCID: PMC8629134.
72. Qiu F, Liang C-L, Liu H, Zeng Y-Q, Hou S, Huang S, Lai X, Dai Z. Impacts of cigarette smoking on immune responsiveness: Up and down or upside down? Oncotarget. 2017;8(1):268-84. doi: 10.18632/oncotarget.13613. PubMed PMID: 27902485.
73. Brody AL, Hubert R, Enoki R, Garcia LY, Mamoun MS, Okita K, London ED, Nurmi EL, Seaman LC, Mandelkern MA. Effect of Cigarette Smoking on a Marker for Neuroinflammation: A [(11)C]DAA1106 Positron Emission Tomography Study. Neuropsychopharmacology : official publication of the American College of Neuropsychopharmacology. 2017;42(8):1630-9. Epub 2017/03/07. doi: 10.1038/npp.2017.48. PubMed PMID: 28262740; PMCID: PMC5518907.
74. Adeluyi A, Guerin L, Fisher ML, Galloway A, Cole RD, Chan SSL, Wyatt MD, Davis SW, Freeman LR, Ortinski PI, Turner JR. Microglia morphology and proinflammatory signaling in the nucleus accumbens during nicotine withdrawal. Sci Adv. 2019;5(10):eaax7031-eaax. doi: 10.1126/sciadv.aax7031. PubMed PMID: 31633029.
75. Kadry H, Noorani B, Cucullo L. A blood–brain barrier overview on structure, function, impairment, and biomarkers of integrity. Fluids and Barriers of the CNS. 2020;17(1):69. doi: 10.1186/s12987-020-00230-3.
76. Engelhardt B. Development of the blood-brain barrier. Cell Tissue Res. 2003;314(1):119-29. Epub 2003/09/05. doi: 10.1007/s00441-003-0751-z. PubMed PMID: 12955493.
77. Ghosh C, Puvenna V, Gonzalez-Martinez J, Janigro D, Marchi N. Blood-brain barrier P450 enzymes and multidrug transporters in drug resistance: a synergistic role in neurological diseases. Curr

Drug Metab. 2011;12(8):742-9. Epub 2011/05/17. doi: 10.2174/138920011798357051. PubMed PMID: 21568937; PMCID: PMC4874186.
78. Nakagomi T, Kubo S, Nakano-Doi A, Sakuma R, Lu S, Narita A, Kawahara M, Taguchi A, Matsuyama T. Brain vascular pericytes following ischemia have multipotential stem cell activity to differentiate into neural and vascular lineage cells. Stem Cells. 2015;33(6):1962-74. Epub 2015/02/20. doi: 10.1002/stem.1977. PubMed PMID: 25694098.
79. Sofroniew MV, Vinters HV. Astrocytes: biology and pathology. Acta Neuropathol. 2010;119(1):7-35. Epub 2009/12/17. doi: 10.1007/s00401-009-0619-8. PubMed PMID: 20012068; PMCID: PMC2799634.
80. Pun PB, Lu J, Moochhala S. Involvement of ROS in BBB dysfunction. Free Radic Res. 2009;43(4):348-64. Epub 2009/02/26. doi: 10.1080/10715760902751902. PubMed PMID: 19241241.
81. Hossain M, Sathe T, Fazio V, Mazzone P, Weksler B, Janigro D, Rapp E, Cucullo L. Tobacco smoke: a critical etiological factor for vascular impairment at the blood-brain barrier. Brain Res. 2009;1287:192-205. Epub 2009/06/23. doi: 10.1016/j.brainres.2009.06.033. PubMed PMID: 19539613; PMCID: PMC2831230.
82. Abbruscato TJ, Lopez SP, Mark KS, Hawkins BT, Davis TP. Nicotine and cotinine modulate cerebral microvascular permeability and protein expression of ZO-1 through nicotinic acetylcholine receptors expressed on brain endothelial cells. J Pharm Sci. 2002;91(12):2525-38. Epub 2002/11/16. doi: 10.1002/jps.10256. PubMed PMID: 12434396.
83. Abbruscato TJ, Lopez SP, Roder K, Paulson JR. Regulation of blood-brain barrier Na,K,2Cl-cotransporter through phosphorylation during in vitro stroke conditions and nicotine exposure. J Pharmacol Exp Ther. 2004;310(2):459-68. Epub 2004/04/03. doi: 10.1124/jpet.104.066274. PubMed PMID: 15051802.
84. Pun PBL, Lu J, Moochhala S. Involvement of ROS in BBB dysfunction. Free Radical Research. 2009;43(4):348-64. doi: 10.1080/10715760902751902.
85. Pizzino G, Irrera N, Cucinotta M, Pallio G, Mannino F, Arcoraci V, Squadrito F, Altavilla D, Bitto A. Oxidative Stress: Harms and Benefits for Human Health. Oxid Med Cell Longev. 2017;2017:8416763-. Epub 2017/07/27. doi: 10.1155/2017/8416763. PubMed PMID: 28819546.
86. Salim S. Oxidative Stress and the Central Nervous System. J Pharmacol Exp Ther. 2017;360(1):201-5. Epub 2016/10/17. doi: 10.1124/jpet.116.237503. PubMed PMID: 27754930.
87. Wang X, Michaelis EK. Selective neuronal vulnerability to oxidative stress in the brain. Front Aging Neurosci. 2010;2:12. Epub 2010/06/17. doi: 10.3389/fnagi.2010.00012. PubMed PMID: 20552050; PMCID: PMC2874397.
88. Ge T, Yang J, Zhou S, Wang Y, Li Y, Tong X. The Role of the Pentose Phosphate Pathway in Diabetes and Cancer. Frontiers in Endocrinology. 2020;11. doi: 10.3389/fendo.2020.00365.
89. Kleinridders A, Ferris HA, Reyzer ML, Rath M, Soto M, Manier ML, Spraggins J, Yang Z, Stanton RC, Caprioli RM, Kahn CR. Regional differences in brain glucose metabolism determined by imaging mass spectrometry. Molecular Metabolism. 2018;12:113-21. doi: https://doi.org/10.1016/j.molmet.2018.03.013.
90. Moon SJ, Dong W, Stephanopoulos GN, Sikes HD. Oxidative pentose phosphate pathway and glucose anaplerosis support maintenance of mitochondrial NADPH pool under mitochondrial oxidative stress. Bioeng Transl Med. 2020;5(3):e10184-e. doi: 10.1002/btm2.10184. PubMed PMID: 33005744.
91. Pandolfi PP, Sonati F, Rivi R, Mason P, Grosveld F, Luzzatto L. Targeted disruption of the housekeeping gene encoding glucose 6-phosphate dehydrogenase (G6PD): G6PD is dispensable for pentose synthesis but essential for defense against oxidative stress. Embo j. 1995;14(21):5209-15. Epub 1995/11/01. PubMed PMID: 7489710; PMCID: PMC394630.

92. Brodaty H, Breteler MM, Dekosky ST, Dorenlot P, Fratiglioni L, Hock C, Kenigsberg PA, Scheltens P, De Strooper B. The world of dementia beyond 2020. J Am Geriatr Soc. 2011;59(5):923-7. Epub 2011/04/15. doi: 10.1111/j.1532-5415.2011.03365.x. PubMed PMID: 21488846.
93. Breijyeh Z, Karaman R. Comprehensive Review on Alzheimer's Disease: Causes and Treatment. Molecules. 2020;25(24):5789. doi: 10.3390/molecules25245789. PubMed PMID: 33302541.
94. Knopman DS, Amieva H, Petersen RC, Chételat G, Holtzman DM, Hyman BT, Nixon RA, Jones DT. Alzheimer disease. Nature Reviews Disease Primers. 2021;7(1):33. doi: 10.1038/s41572-021-00269-y.
95. Overk CR, Masliah E. Pathogenesis of synaptic degeneration in Alzheimer's disease and Lewy body disease. Biochem Pharmacol. 2014;88(4):508-16. Epub 2014/01/28. doi: 10.1016/j.bcp.2014.01.015. PubMed PMID: 24462903; PMCID: PMC3973539.
96. Cataldo JK, Prochaska JJ, Glantz SA. Cigarette smoking is a risk factor for Alzheimer's Disease: an analysis controlling for tobacco industry affiliation. J Alzheimers Dis. 2010;19(2):465-80. Epub 2010/01/30. doi: 10.3233/jad-2010-1240. PubMed PMID: 20110594; PMCID: PMC2906761.
97. Chang C-CH, Zhao Y, Lee C-W, Ganguli M. Smoking, death, and Alzheimer disease: a case of competing risks. Alzheimer Dis Assoc Disord. 2012;26(4):300-6. doi: 10.1097/WAD.0b013e3182420b6e. PubMed PMID: 22185783.
98. Nikon Microscopy U. Introductory Confocal Concepts 2022. Available from: https://www.microscopyu.com/techniques/confocal/introductory-confocal-concepts.
99. Chen X, Nadiarynkh O, Plotnikov S, Campagnola PJ. Second harmonic generation microscopy for quantitative analysis of collagen fibrillar structure. Nature Protocols. 2012;7(4):654-69. doi: 10.1038/nprot.2012.009.
100. Pantazis P, Maloney J, Wu D, Fraser SE. Second harmonic generating (SHG) nanoprobes for in vivo imaging. Proc Natl Acad Sci U S A. 2010;107(33):14535-40. Epub 2010/07/30. doi: 10.1073/pnas.1004748107. PubMed PMID: 20668245; PMCID: PMC2930484 filed by the California Institute of Technology.
101. Choo YW, Jeong J, Jung K. Recent advances in intravital microscopy for investigation of dynamic cellular behavior in vivo. BMB Rep. 2020;53(7):357-66. doi: 10.5483/BMBRep.2020.53.7.069. PubMed PMID: 32475382.
102. Derk J, Jones HE, Como C, Pawlikowski B, Siegenthaler JA. Living on the Edge of the CNS: Meninges Cell Diversity in Health and Disease. Front Cell Neurosci. 2021;15:703944. Epub 2021/07/20. doi: 10.3389/fncel.2021.703944. PubMed PMID: 34276313; PMCID: PMC8281977.
103. Vaghela R, Arkudas A, Horch RE, Hessenauer M. Actually Seeing What Is Going on – Intravital Microscopy in Tissue Engineering. Frontiers in Bioengineering and Biotechnology. 2021;9. doi: 10.3389/fbioe.2021.627462.
104. Yang G, Pan F, Parkhurst CN, Grutzendler J, Gan W-B. Thinned-skull cranial window technique for long-term imaging of the cortex in live mice. Nature protocols. 2010;5(2):201-8. Epub 2010/01/14. doi: 10.1038/nprot.2009.222. PubMed PMID: 20134419.
105. Benisty H, Song A, Mishne G, Charles As. Data Processing of Functional Optical Microscopy for Neuroscience2022.
106. Shih C-T, Chen N-Y, Wang T-Y, He G-W, Wang G-T, Lin Y-J, Lee T-K, Chiang A-S. NeuroRetriever: Automatic Neuron Segmentation for Connectome Assembly. Frontiers in Systems Neuroscience. 2021;15. doi: 10.3389/fnsys.2021.687182.
107. Magliaro C, Callara AL, Vanello N, Ahluwalia A. Gotta Trace 'em All: A Mini-Review on Tools and Procedures for Segmenting Single Neurons Toward Deciphering the Structural Connectome. Frontiers in Bioengineering and Biotechnology. 2019;7. doi: 10.3389/fbioe.2019.00202.
108. Derby KS, Cuthrell K, Caberto C, Carmella S, Murphy SE, Hecht SS, Le Marchand L. Exposure to the carcinogen 4-(methylnitrosamino)-1-(3-pyridyl)-1-butanone (NNK) in smokers from 3 populations

with different risks of lung cancer. Int J Cancer. 2009;125(10):2418-24. doi: 10.1002/ijc.24585. PubMed PMID: 19598261.
109. Ghosh D, Mishra MK, Das S, Kaushik DK, Basu A. Tobacco carcinogen induces microglial activation and subsequent neuronal damage. Journal of neurochemistry. 2009;110(3):1070-81. Epub 2009/06/09. doi: 10.1111/j.1471-4159.2009.06203.x. PubMed PMID: 19500213.
110. Hecht SS, Trushin N, Rigotty J, Carmella SG, Borukhova A, Akerkar S, Rivenson A. Complete inhibition of 4-(methylnitrosamino)-1-(3-pyridyl)-1-butanone-induced rat lung tumorigenesis and favorable modification of biomarkers by phenethyl isothiocyanate. Cancer Epidemiol Biomarkers Prev. 1996;5(8):645-52. Epub 1996/08/01. PubMed PMID: 8824368.
111. Hoffmann D, Rivenson A, Amin S, Hecht SS. Dose-response study of the carcinogenicity of tobacco-specific N-nitrosamines in F344 rats. J Cancer Res Clin Oncol. 1984;108(1):81-6. Epub 1984/01/01. doi: 10.1007/bf00390978. PubMed PMID: 6746721.
112. Wei B, Blount BC, Xia B, Wang L. Assessing exposure to tobacco-specific carcinogen NNK using its urinary metabolite NNAL measured in US population: 2011-2012. J Expo Sci Environ Epidemiol. 2016;26(3):249-56. Epub 2015/01/08. doi: 10.1038/jes.2014.88. PubMed PMID: 25564369; PMCID: PMC4520776.
113. Park YG, Sohn CH, Chen R, McCue M, Yun DH, Drummond GT, Ku T, Evans NB, Oak HC, Trieu W, Choi H, Jin X, Lilascharoen V, Wang J, Truttmann MC, Qi HW, Ploegh HL, Golub TR, Chen SC, Frosch MP, Kulik HJ, Lim BK, Chung K. Protection of tissue physicochemical properties using polyfunctional crosslinkers. Nat Biotechnol. 2018. Epub 2018/12/18. doi: 10.1038/nbt.4281. PubMed PMID: 30556815; PMCID: PMC6579717.
114. Yun DH, Park Y-G, Cho JH, Kamentsky L, Evans NB, Albanese A, Xie K, Swaney J, Sohn CH, Tian Y, Zhang Q, Drummond G, Guan W, DiNapoli N, Choi H, Jung H-Y, Ruelas L, Feng G, Chung K. Ultrafast immunostaining of organ-scale tissues for scalable proteomic phenotyping. bioRxiv. 2019:660373. doi: 10.1101/660373.
115. Preibisch S, Saalfeld S, Tomancak P. Globally optimal stitching of tiled 3D microscopic image acquisitions. Bioinformatics. 2009;25(11):1463-5. Epub 2009/04/03. doi: 10.1093/bioinformatics/btp184. PubMed PMID: 19346324.
116. Bowyer JF, Sarkar S, Burks SM, Hess JN, Tolani S, O'Callaghan JP, Hanig JP. Microglial activation and responses to vasculature that result from an acute LPS exposure. Neurotoxicology. 2020;77:181-92. Epub 2020/01/31. doi: 10.1016/j.neuro.2020.01.014. PubMed PMID: 32014511.
117. Sharpe D. Chi-Square Test is Statistically Significant: Now What? Practical Assessment, Research, and Evaluation. 2015;20. doi: https://doi.org/10.7275/tbfa-x148.
118. Prevention CfDCa. Health Effects of Cigarette Smoking 2019. Available from: https://www.cdc.gov/tobacco/data_statistics/fact_sheets/health_effects/effects_cig_smoking/index.htm.
119. Hu S-C, Min S, Kang H-K, Yang D-J, Basavarajappa M, Lewis SM, Davis KJ, Patton RE, Bryant MS, Sepehr E, Trbojevich R, Pearce MG, Bishop ME, Ding W, Heflich RH, Maisha MP, Felton R, Chemerynski S, Yee SB, Coraggio M, Rosenfeldt H, Yeager RP, Howard PC, Tang Y. 90-day nose-only inhalation toxicity study of 4-(methylnitrosamino)-1-(3-pyridyl)-1-butanone (NNK) in Sprague-Dawley rats. Food and Chemical Toxicology. 2022;160:112780. doi: https://doi.org/10.1016/j.fct.2021.112780.
120. Lull ME, Block ML. Microglial activation and chronic neurodegeneration. Neurotherapeutics : the journal of the American Society for Experimental NeuroTherapeutics. 2010;7(4):354-65. Epub 2010/10/01. doi: 10.1016/j.nurt.2010.05.014. PubMed PMID: 20880500; PMCID: PMC2951017.
121. Sweeney MD, Sagare AP, Zlokovic BV. Blood-brain barrier breakdown in Alzheimer disease and other neurodegenerative disorders. Nature reviews Neurology. 2018;14(3):133-50. Epub 2018/01/30. doi: 10.1038/nrneurol.2017.188. PubMed PMID: 29377008; PMCID: PMC5829048.

122. Bernacki J, Dobrowolska A, Nierwinska K, Malecki A. Physiology and pharmacological role of the blood-brain barrier. Pharmacological reports : PR. 2008;60(5):600-22. Epub 2008/12/11. PubMed PMID: 19066407.
123. Hirata N, Yamada S, Sekino Y, Kanda Y. Tobacco nitrosamine NNK increases ALDH-positive cells via ROS-Wnt signaling pathway in A549 human lung cancer cells. The Journal of Toxicological Sciences. 2017;42(2):193-204. doi: 10.2131/jts.42.193.
124. Zhao X, Eyo UB, Murugan M, Wu L-J. Microglial interactions with the neurovascular system in physiology and pathology. Dev Neurobiol. 2018;78(6):604-17. Epub 2018/02/01. doi: 10.1002/dneu.22576. PubMed PMID: 29318762.
125. Koizumi T, Kerkhofs D, Mizuno T, Steinbusch HWM, Foulquier S. Vessel-Associated Immune Cells in Cerebrovascular Diseases: From Perivascular Macrophages to Vessel-Associated Microglia. Front Neurosci. 2019;13:1291-. doi: 10.3389/fnins.2019.01291. PubMed PMID: 31866808.
126. Chaudhry R MJ, Rehman A. Physiology, Cardiovascular. In: StatPearls [Internet]. Treasure Island (FL): StatPearls Publishing; 2021 [cited 2022 January]. Available from: https://www.ncbi.nlm.nih.gov/books/NBK493197/.
127. World Health Organization. Tobacco 2021 [updated July 26, 2021]. Available from: https://www.who.int/news-room/fact-sheets/detail/tobacco.
128. Doukas SG, Vageli DP, Lazopoulos G, Spandidos DA, Sasaki CT, Tsatsakis A. The Effect of NNK, A Tobacco Smoke Carcinogen, on the miRNA and Mismatch DNA Repair Expression Profiles in Lung and Head and Neck Squamous Cancer Cells. Cells. 2020;9(4):1031. PubMed PMID: doi:10.3390/cells9041031.
129. Yalcin E, de la Monte S. Tobacco nitrosamines as culprits in disease: mechanisms reviewed. J Physiol Biochem. 2016;72(1):107-20. Epub 2016/01/14. doi: 10.1007/s13105-016-0465-9. PubMed PMID: 26767836.
130. Lee H-W, Park S-H, Weng M-w, Wang H-T, Huang WC, Lepor H, Wu X-R, Chen L-C, Tang M-s. E-cigarette smoke damages DNA and reduces repair activity in mouse lung, heart, and bladder as well as in human lung and bladder cells. Proceedings of the National Academy of Sciences. 2018;115(7):E1560-E9. doi: 10.1073/pnas.1718185115.
131. Jorquera R, Castonguay A, Schuller HM. Placental transfer of 4-(methylnitrosamino)-1-(3-pyridyl)-1-butanone instilled intratracheally in Syrian golden hamsters. Cancer Res. 1992;52(12):3273-80. Epub 1992/06/15. PubMed PMID: 1596885.
132. Varatharaj A, Galea I. The blood-brain barrier in systemic inflammation. Brain, Behavior, and Immunity. 2017;60:1-12. doi: https://doi.org/10.1016/j.bbi.2016.03.010.
133. Ly TT, Wang J, Bisht K, Eyo U, Acton ST. C3VFC: A Method for Tracing and Quantification of Microglia in 3D Temporal Images. Applied Sciences. 2021;11(13):6078. PubMed PMID: doi:10.3390/app11136078.
134. York EM, LeDue JM, Bernier L-P, MacVicar BA. 3DMorph Automatic Analysis of Microglial Morphology in Three Dimensions from Ex Vivo and In Vivo Imaging. eNeuro. 2018;5(6):ENEURO.0266-18.2018. doi: 10.1523/ENEURO.0266-18.2018. PubMed PMID: 30627639.
135. Lively S, Schlichter LC. The microglial activation state regulates migration and roles of matrix-dissolving enzymes for invasion. J Neuroinflammation. 2013;10:75. Epub 2013/06/22. doi: 10.1186/1742-2094-10-75. PubMed PMID: 23786632; PMCID: PMC3693964.
136. Miller EB, Zhang P, Ching K, Pugh EN, Jr., Burns ME. In vivo imaging reveals transient microglia recruitment and functional recovery of photoreceptor signaling after injury. Proc Natl Acad Sci U S A. 2019;116(33):16603-12. Epub 2019/07/28. doi: 10.1073/pnas.1903336116. PubMed PMID: 31350349; PMCID: PMC6697899.
137. Bisht K, Okojie KA, Sharma K, Lentferink DH, Sun Y-Y, Chen H-R, Uweru JO, Amancherla S, Calcuttawala Z, Campos-Salazar AB, Corliss B, Jabbour L, Benderoth J, Friestad B, Mills WA, Isakson BE, Tremblay M-È, Kuan C-Y, Eyo UB. Capillary-associated microglia regulate vascular structure and function

through PANX1-P2RY12 coupling in mice. Nature Communications. 2021;12(1):5289. doi: 10.1038/s41467-021-25590-8.
138. Morsch M, Radford R, Lee A, Don E, Badrock A, Hall T, Cole N, Chung R. In vivo characterization of microglial engulfment of dying neurons in the zebrafish spinal cord. Frontiers in Cellular Neuroscience. 2015;9. doi: 10.3389/fncel.2015.00321.
139. Smith JA, Das A, Ray SK, Banik NL. Role of pro-inflammatory cytokines released from microglia in neurodegenerative diseases. Brain Research Bulletin. 2012;87(1):10-20. doi: https://doi.org/10.1016/j.brainresbull.2011.10.004.
140. Bennett RE, Robbins AB, Hu M, Cao X, Betensky RA, Clark T, Das S, Hyman BT. Tau induces blood vessel abnormalities and angiogenesis-related gene expression in P301L transgenic mice and human Alzheimer's disease. Proceedings of the National Academy of Sciences. 2018;115(6):E1289. doi: 10.1073/pnas.1710329115.
141. Roy A RI, Jabbour S, et al. Tobacco and Cardiovascular Disease: A Summary of Evidence. . 3rd ed. Prabhakaran D AS, Gaziano TA, et al., editor. Cardiovascular, Respiratory, and Related Disorders.: Washington (DC): The International Bank for Reconstruction and Development / The World Bank; 2017.
142. Min-Liang Si TJFL. Nicotinic Acetylcholine Receptors on Cerebral Perivascular Sympathetic Nerves Mediate Choline-Induced Nitrergic Neurogenic Vasodilation. Circulation Research. 2002;91(1):62-9. doi: doi:10.1161/01.RES.0000024417.79275.23.
143. Zou Q, Leung SW, Vanhoutte PM. Activation of nicotinic receptors can contribute to endothelium-dependent relaxations to acetylcholine in the rat aorta. J Pharmacol Exp Ther. 2012;341(3):756-63. Epub 2012/03/20. doi: 10.1124/jpet.112.192229. PubMed PMID: 22427701.
144. Dukart J, Holiga Š, Chatham C, Hawkins P, Forsyth A, McMillan R, Myers J, Lingford-Hughes AR, Nutt DJ, Merlo-Pich E, Risterucci C, Boak L, Umbricht D, Schobel S, Liu T, Mehta MA, Zelaya FO, Williams SC, Brown G, Paulus M, Honey GD, Muthukumaraswamy S, Hipp J, Bertolino A, Sambataro F. Cerebral blood flow predicts differential neurotransmitter activity. Sci Rep. 2018;8(1):4074. Epub 2018/03/08. doi: 10.1038/s41598-018-22444-0. PubMed PMID: 29511260; PMCID: PMC5840131 current or former full-time employees of F.Hoffmann-La Roche, Basel Switzerland. The authors received no specific funding for this work. F.Hoffmann-La Roche provided financial contribution in the form of salary for all authors listed above but did not have any additional role in the study design, data collection and analysis, decision to publish, or preparation of the manuscript.
145. Jamjoom AAB, Rhodes J, Andrews PJD, Grant SGN. The synapse in traumatic brain injury. Brain. 2021;144(1):18-31. Epub 2020/11/14. doi: 10.1093/brain/awaa321. PubMed PMID: 33186462; PMCID: PMC7880663.
146. Lee E, Chung W-S. Glial Control of Synapse Number in Healthy and Diseased Brain. Frontiers in cellular neuroscience. 2019;13:42-. doi: 10.3389/fncel.2019.00042. PubMed PMID: 30814931.
147. Coley AA, Gao WJ. PSD-95 deficiency disrupts PFC-associated function and behavior during neurodevelopment. Sci Rep. 2019;9(1):9486. Epub 2019/07/03. doi: 10.1038/s41598-019-45971-w. PubMed PMID: 31263190; PMCID: PMC6602948.
148. Dore K, Carrico Z, Alfonso S, Marino M, Koymans K, Kessels HW, Malinow R. PSD-95 protects synapses from β-amyloid. Cell Rep. 2021;35(9):109194. Epub 2021/06/03. doi: 10.1016/j.celrep.2021.109194. PubMed PMID: 34077732; PMCID: PMC8237704.
149. Zheng H-C, Takano Y. NNK-Induced Lung Tumors: A Review of Animal Model. J Oncol. 2011;2011:635379-. Epub 2011/04/27. doi: 10.1155/2011/635379. PubMed PMID: 21559252.
150. Díez-Izquierdo A, Cassanello-Peñarroya P, Lidón-Moyano C, Matilla-Santander N, Balaguer A, Martínez-Sánchez JM. Update on thirdhand smoke: A comprehensive systematic review. Environ Res. 2018;167:341-71. Epub 2018/08/11. doi: 10.1016/j.envres.2018.07.020. PubMed PMID: 30096604.
151. Kassem NO, Daffa RM, Liles S, Jackson SR, Kassem NO, Younis MA, Mehta S, Chen M, Jacob P, 3rd, Carmella SG, Chatfield DA, Benowitz NL, Matt GE, Hecht SS, Hovell MF. Children's exposure to

secondhand and thirdhand smoke carcinogens and toxicants in homes of hookah smokers. Nicotine Tob Res. 2014;16(7):961-75. Epub 2014/03/05. doi: 10.1093/ntr/ntu016. PubMed PMID: 24590387; PMCID: PMC4072898.

152. Matt GE, Quintana PJE, Zakarian JM, Hoh E, Hovell MF, Mahabee-Gittens M, Watanabe K, Datuin K, Vue C, Chatfield DA. When smokers quit: exposure to nicotine and carcinogens persists from thirdhand smoke pollution. Tob Control. 2016;26(5):548-56. Epub 2016/09/23. doi: 10.1136/tobaccocontrol-2016-053119. PubMed PMID: 27655249; PMCID: PMC6478602.

153. Schick SF, Farraro KF, Perrino C, Sleiman M, van de Vossenberg G, Trinh MP, Hammond SK, Jenkins BM, Balmes J. Thirdhand cigarette smoke in an experimental chamber: evidence of surface deposition of nicotine, nitrosamines and polycyclic aromatic hydrocarbons and de novo formation of NNK. Tob Control. 2014;23(2):152-9. Epub 2013/05/30. doi: 10.1136/tobaccocontrol-2012-050915. PubMed PMID: 23716171.